ARTICLE
Journal of Cellular Biochemistry 116:903–922 (2015)

Journal of Cellular Biochemistry

Characterisation of the Kynurenine Pathway in Skin-Derived Fibroblasts and Keratinocytes

Diba Sheipouri,[1] Ross Grant,[1,2] Sonia Bustamante,[3] David Lovejoy,[4] Gilles J. Guillemin,[4,5]* and Nady Braidy[6]**

[1]*Department of Pharmacology, School of Medical Sciences, Faculty of Medicine, University of New South Wales, Sydney, Australia*

[2]*Australasian Research Institute, Sydney Adventist Hospital, Sydney, Australia*

[3]*Bioanalytical Mass Spectrometry Facility, University of New South Wales, Sydney, Australia*

[4]*Neuropharmacology group, MND and Neurodegenerative Diseases Research Centre, Macquarie University, NSW, Australia*

[5]*St. Vincent's Centre for Applied Medical Research, Sydney, Australia*

[6]*Centre for Healthy Brain Ageing, School of Psychiatry, Faculty of Medicine, University of New South Wales, Sydney, Australia*

ABSTRACT

Acute UVB exposure triggers inflammation leading to the induction of indoleamine 2,3 dioxygenase (IDO1), one of the first enzymes in the kynurenine pathway (KP) for tryptophan degradation. However, limited studies have been undertaken to determine the catabolism of tryptophan within the skin. The aim of this study was two fold: (1) to establish if the administration of the proinflammatory cytokine interferon-gamma (IFN-γ) and/or UVB radiation elicits differential KP expression patterns in human fibroblast and keratinocytes; and (2) to evaluate the effect of KP metabolites on intracellular nicotinamide adenine dinucleotide (NAD^+) levels, and cell viability. Primary cultures of human fibroblasts and keratinocytes were used to examine expression of the KP at the mRNA level using qPCR, and at the protein level using immunocytochemistry. Cellular responses to KP metabolites were assessed by examining extracellular lactate dehydrogenase (LDH) activity and intracellular NAD^+ levels. Major downstream KP metabolites were analyzed using GC/MS and HPLC. Our data shows that the KP is fully expressed both in human fibroblasts and keratinocytes. Exposure to UVB radiation and/or IFN-γ causes significant changes in the expression pattern of downstream KP metabolites and enzymes. Exposure to various concentrations of KP metabolites showed marked differences in cell viability and intracellular NAD^+ production, providing support for involvement of the KP in the de novo synthesis of NAD^+ in the skin. This new information will have a significant impact on our understanding of the pathogenesis of UV related skin damage and the diagnosis of KP related disease states. J. Cell. Biochem. 116: 903–922, 2015. © 2015 Wiley Periodicals, Inc.

KEY WORDS: KYNURENINE; INFLAMMATION; UVB

INTRODUCTION

The kynurenine pathway (KP) is the principal route of catabolism of the essential amino acid L-tryptophan (TRYP), leading to the production of several neurotoxic, immunomodulatory, and neuroprotective metabolites [Bender and McCreanor, 1982; Harris et al., 1998] (Fig. 1). Much of the initial interest in the KP was placed on its role for the de novo synthesis of the essential pyridine nucleotide, nicotinamide adenine dinucleotide (NAD^+). Alternatively, NAD^+ can also be produced from the amide and acid forms of

Gilles J. Guillemin and Nady Braidy shared senior authorship

Grant sponsor: National Health and Medical Research Council; Grant sponsor: The Curran Foundation; Grant sponsor: Rebecca Cooper foundation.

*Correspondence to: Prof. Gilles J. Guillemin, Neuropharmacology group, MND and Neurodegenerative diseases Research Centre, Macquarie University, NSW 2109, Australia. E-mail: gilles.guillemin@mq.edu.au

**Correspondence to: Nady Braidy, Centre for Healthy Brain Ageing, School of Psychiatry, University of New South Wales, Faculty of Medicine, Sydney 2052, Australia. E-mail: n.braidy@unsw.edu.au

Manuscript Received: 11 March 2014; Manuscript Accepted: 13 November 2014

Accepted manuscript online in Wiley Online Library (wileyonlinelibrary.com): 12 January 2015

DOI 10.1002/jcb.25019 • © 2015 Wiley Periodicals, Inc.

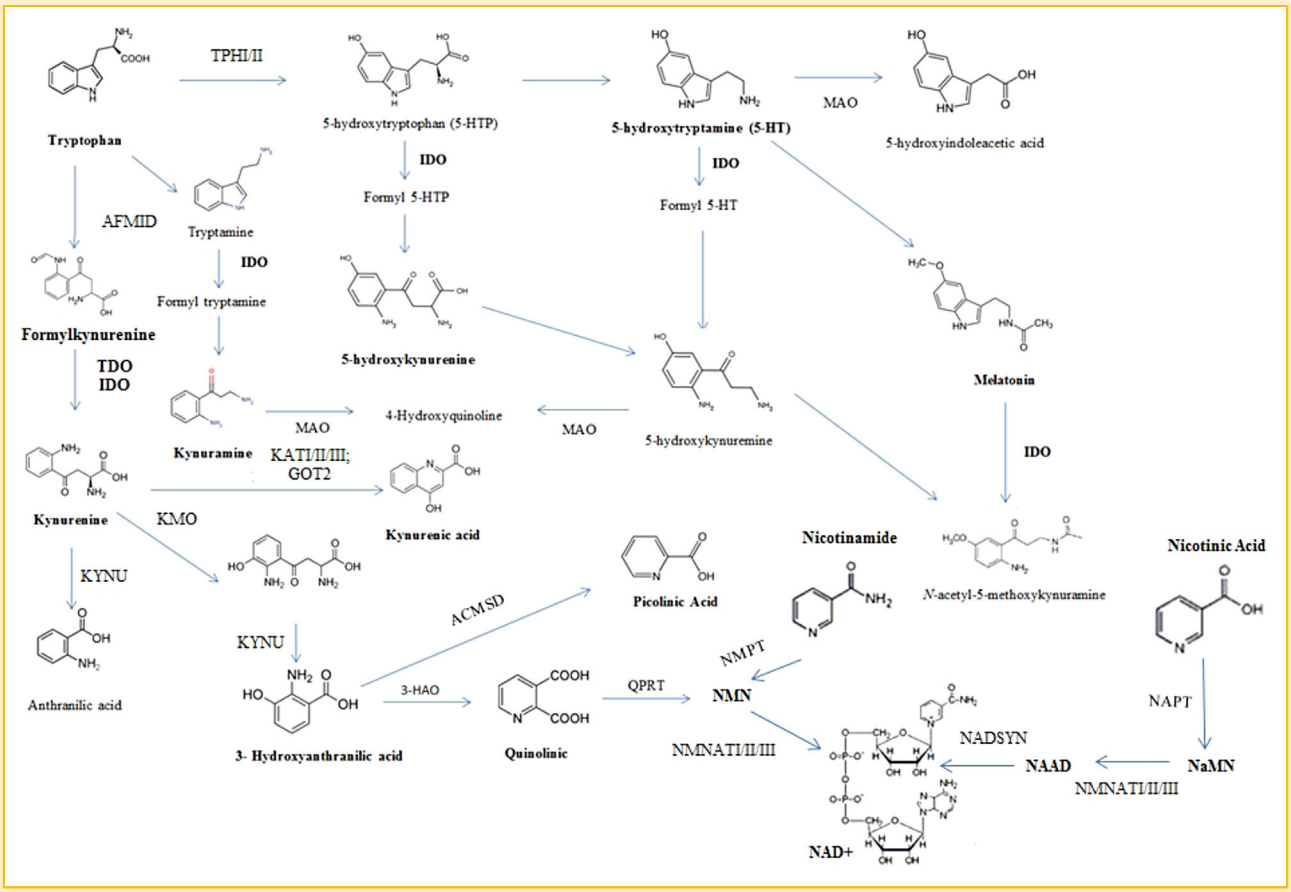

Fig. 1. Pathways for tryptophan metabolism. Dietary tryptophan not used in protein synthesis is metabolized along the kynurenine pathway. Alternatively, tryptophan can also be converted into 5-hydroxytryptamine (5-HT) and then to melatonin, or to tryptamine and then to the kynuramines (or kynurenamines). IDO, indoleamine 2,3 dioxygenase; TDO, tryptophan 2,3 dioxygenase; KYNU, kynureninase; KAT I, kynurenine aminotransferase I; KAT II, kynurenine aminotransferase II; KAT III, kynurenine aminotransferase III; MAO, monoamine oxidase; KMO, kynurenine 3-hydroxylase; GOT2, aspartate aminotransferase; QPRT, quinolinic acid phosphoribosyl transferase; 3-HAA, 3-hydroxyanthranilate 3,4-dioxygenase; TPH I, tryptophan hydroxylase I; THP II, tryptophan hydroxylase II; AFMID, arylformamidase; ACMSD, aminocarboxymuconate semialdehyde decarboxylase; NMNAT-I, nicotinamide mononucleotide adenyl transferase I; NMNAT-II, nicotinamide mononucleotide adenyl transferase II; NMNAT-III, nicotinamide mononucleotide adenyl transferase III; NADSYN, nicotinamide adenine dinucleotide synthase; NAPT, nicotinic acid phosphoribosyl transferase; and NMPT, nicotinamide phosphoribosyl transferase.

vitamin B3 (nicotinamide and nicotinic acid) via the NAD^+ salvage pathway. The discovery of several KP metabolites possessing immunoactive properties has drawn considerable attention to the KP's role in the biology of ageing, including neurodegeneration and other age-related pathologies. Stone and Perkins (1981) showed that quinolinic acid (QUIN) is a potent neurotoxin and selective agonist at N-methyl-D-aspartate (NMDA) glutamate receptors. It was later shown that two other metabolites of the KP, kynurenine (KYN) and kynurenic acid (KYNA), do not show excitotoxic behaviour and that KYNA is in fact a non-selective antagonist at glutamate receptors and is able to block the neurotoxic effects of QUIN [Perkins and Stone, 1982; Kapoor et al., 1994; Jhamandas et al., 2000]. However, KYNA is produced in too little amounts to have any biological protective significance [Boegman et al., 1985]. However, another endogenous metabolite, picolinic acid (PIC) can antagonise the excitotoxic effects of QUIN without affecting its neurotoxic effects through an undetermined mechanism [Jhamandas et al., 1990, 2000]

Activated by interferon gamma [Daubener and MacKenzie, 1999] indoleamine-2,3-dioxygenase (IDO1) is one of the first enzymes triggering the activation of the KP and is responsible for the oxidative metabolism of TRYP [Thomas and Stocker, 1999; Fujigaki et al., 2006]. It has already been shown that human fetal skin fibroblasts and keratinocytes express IDO1 and produce kynurenine. Cells expressing IDO1 have the ability to supress T-cell responses, and hence to induce immune tolerance [Fallarino et al., 2002; Terness et al., 2002; Bauer et al., 2005; Wainwright et al., 2012], which is of great significance in suppressing rejection of allogeneic foetuses during pregnancy [Munn et al., 1998]. IFN-γ-induced IDO expression in skin cells in a co-culture system can suppress the proliferation of peripheral blood mononuclear cells [Sarkhos et al., 2003]. Moreover, upregulation of IDO1 in a subset of T-cell inflamed melanoma tumors may promote tumor escape from immune-mediated destruction [Spranger et al., 2013]. It has already been firmly established that metabolites of the KP also play a vital role in protection against UVB radiation in the human eye

[Tsentalovich et al., 2006; Sherin et al., 2009]. Although these correlations in biochemical physiology have been very widely recognized, research aiming to draw correlations between aberrations in the KP and acute UVB exposure in the skin, is currently lacking.

UVB damage in the skin is a very common phenomenon in which repeated exposure triggers inflammation, leading to the loss of elasticity and wrinkle formation [Akazaki and Imokawa, 2001]. The KP has been previously shown to be deregulated in several inflammatory diseases and acute UVB exposure has been shown to include an inflammatory component, which may induce IDO1. Moreover, the KP has recently been shown to be expressed in human dermal fibroblasts, although the significance of this pathway in immunosurveillance and cellular metabolism remains unclear [Asp et al., 2011]. Therefore, in this study we aimed to establish: (1) whether or not the KP was fully expressed in both human foetal skin-derived fibroblasts and keratinocytes; and (2) whether the administration of the proinflammatory cytokine IFN-γ, and/or exposure to UVB radiation can elicit differences in the expression pattern of the KP in the skin.

MATERIALS AND METHODS

ETHICS APPROVAL

Human foetal tissue was obtained following informed written consent. This study has been approved by the Human Ethics Committees (HREC 08284) from the University of New South Wales.

REAGENTS AND CHEMICALS

Dulbecco′s phosphate buffer solution (DPBS) and all other cell culture media and supplements were from Invitrogen (Melbourne, Australia) unless otherwise stated. Nicotinamide, bicine, nicotinamide adenine dinucleotide reduced form (NADH), 3-[-4,5-dimethylthiazol-2-yl]-2,5-diphenyl tetrazolium bromide (MTT), alcohol dehydrogenase (ADH), sodium pyruvate, TRIS buffered saline, trypsin, L-tryptophan (TRP), kynurenine (KYN), kynurenic acid (KYNA), anthranilic acid (AA), 3- hydroxyanthranilic acid (3-HAA), 3-hydroxykynurenine (3-HK), picolinic acid (PIC), and quinolinic acid (QUIN) and 4′,6-Diamidino-2-phenylindole dihydrochloride (DAPI) were obtained from Sigma–Aldrich (Castle-Hill, Australia). Phenazine methosulfate (PMS) was obtained from ICN Biochemicals (Ohio, USA). Bradford reagent was obtained from BioRad, Hercules (California, USA). Interferon gamma was obtained from Boehringer Mannheim (Boehringer Mannheim, Germany). Anti quinolinic acid and anti-cytokeratin rabbit polyclonal antibody (pAb) and, anti-fibronectin mouse mAb were purchased from Millipore (Melbourne, Australia). Anti-IDO-1 mouse mAb, and anti-tryptophan 2, 3-dioxygenase (TDO) rabbit pAb were generously provided by Prof. O. Takikawa, T. Uemura (Psychiatric Research Institute of Tokyo, Japan), and Prof. C. Miller (Johns Hopkins University, Baltimore, MD), respectively. These three antibodies were used at concentrations of 10, 10, and 2 μg/mL, respectively. Polyclonal antibodies for detection of α-amino-β-carboxymuconate-semi-aldehyde decarboxylase (ACMSD), quinolinate phosphoribosyltransferase (QPRT), kynurenine amino transferase-I (KAT I), kynureninase (KYNU), kynurenine 3-monooxygenase (KMO) and nicotinamide mononucleotide adenyltransferase-I, II and III (NMNATI/II/III), were obtained from Abnova (Taipei, Taiwan) and used at a concentration of 2 μg/mL. Alexa 488- or Alexa 594-conjugated anti-mouse IgG or anti-rabbit were purchased from Invitrogen. All commercial antibodies were used at the concentrations recommended by the manufacturer.

UVB LAMP

Ultraviolet B (UVB) irradiation was carried out using a Stratagene 2000 illuminator specially equipped with FG15T8 bulbs, which produce maximal output in the UVB range (290–320 nm).

CELL CULTURES

Human foetal skin cells were obtained from 14–18 week old foetuses collected after therapeutic termination following informed consent. **Fibroblasts.** Skin pieces were washed in 1% DPBS (Invitrogen, Melbourne, Australia) by gently shaking a 50 mL polypropylene centrifuge tube. Samples were placed on a tissue culture lid (epidermal side down) and sliced into strips about 0.5 cm width using a surgical scalpel and then incubated for 20 minutes at 37°C in 0.3% (w/v) trypsin (from bovine pancreas; Sigma) in PBS, and then gently shaken. Samples were then washed again with PBS in a 50 mL polypropylene centrifuge tube. 3–4 mm squares are cut made from the sample using a fine surgical blade and placed into a 75 cm^2 tissue culture flask containing 30 mL of complete growth medium (500 mL DMEM or RPMI, 60 mL FBS (heat-inactivated 60 min at 56°C), 5 mL 1 M HEPES buffer solution, 5 mL 100× nonessential amino acid mixture, 5 mL 100× L-glutamine, 5 mL 100× penicillin/streptomycin, 5 mL 100× sodium pyruvate). The flask was placed into an incubator at 37°C, 5% CO_2 and medium was changed every 3–4 days. **Keratinocytes.** Skin pieces were washed in HEPES buffered saline (Invitrogen, Melbourne, Australia) by gently shaking a 50 mL polypropylene centrifuge tube. Sample were placed on a tissue culture dish (epidermal side up) and sliced into strips about 0.5 cm width using a surgical scalpel. Trypsin (0.25%) was added and incubated at 37°C, 5% CO_2 for 1 h. The epidermis was peeled back using forceps and placed in a tissue culture dish containing 5 mL keratinocyte primary culture medium (Invitrogen, Melbourne, Australia). Cells were released by gently titrating up and down using a disposable 5 mL syringe. The cell suspension was passed through a coarse filter to remove debris and then centrifuged for 5 min at 200 *g* at room temperature. Afterwards, the supernatant was aspirated, and cells are resuspended in 10 mL keratinocyte primary culture medium in a 75 cm^2 cell culture flask. The flask was placed in 37°C, 5% CO_2 incubator overnight and washed gently with Hanks balanced salt solution (Invitrogen), followed by the addition of 15 mL keratinocyte primary culture medium. The medium was changed every second day until cells reached about 70–80% confluence.

IMMUNOCYTOCHEMISTRY

Human foetal fibroblasts and keratinocytes were grown in Permanox chamber slides for 2–3 days. After 72 h, untreated, UVB treated and IFN-γ treated cells were fixed with methanol/ acetone (1:1) v/v for 20 min at −20°C. Cells were then washed three times with PBS and

incubated with 0.025% Triton X-100 (Invitrogen, Melbourne, Australia) in PBS for 10 min at 22°C to create membrane permeability. Cells were washed and incubated with 5% (v/v) non-immune goat serum (NGS) in PBS for 45 min at 22°C, rinsed twice with PBS and incubated for 1 h at 37°C with the primary mAb or pAb antibodies that had been diluted in 5% NGS (Supplementary Table SI). Following this incubation, cells were washed again with 5% NGS solution and incubated at 37°C with the appropriate secondary antibody (goat anti mouse IgG or goat anti rabbit IgG coupled to Alexa 488 or Alexa 594). 1 g/mL DAPI for 5 min at 22°C was used for nuclear staining then washed several times with in PBS at 37°C. Coverslips were then mounted using Fluoromount-G and examined using an Olympus BX60 fluorescence microscope fitted with a SensiCam digital camera. Three controls were performed for each immunolabelling experiment: (1) isotypic antibody controls for mAbs and serum control for pAbs; (2) incubation with only the secondary labelled antibodies; and (3) measurement of autofluorescence of unlabelled cells.

For immunofluorescence staining of KP constituents in tissue, skin whole mounts were immersion-fixed with ice cold 70% ethanol for 20 min followed by 4% paraformaldehyde (PFA), pH 7.4 for 10 min at 4°C. Immunostaining was established on skin whole mount as described above.

HEMATOXYLIN AND EOSIN STAINING

Samples were deparaffinised by washing three times for 5 min in xylene, then taken through two changes of 10 min washes in 100% ethanol, one 10-min wash in 95% ethanol and finally rinsed in dH_20 twice for 5 min each. Slides were brought to a boil in 10 mM sodium citrate buffer solution (pH 6.0) and maintained at sub boiling temperatures for 10 min.

Slides were then over-stained with hematoxylin for 10 min and excess stain is removed by running under tap water for 2 min. Afterwards, they were differentiated and destained by submerging in acid alcohol for a few seconds until sections appeared red then rinsed briefly under tap water to remove acid. Slides were blued in bicarbonate until nuclei stood out significantly then rinsed under tap water for 5 min. Afterwards, the slides were submerged in 70% ethanol for 3 min, and then in eosin for 2 min. The slides were then taken through three changes of 95% ethanol, for 5 min each. Finally, slides were rinsed in 100% ethanol, coverslip and mounted.

FLOW CYTOMETRY

For flow cytometry, 0.2×10^6 cells were stained along with appropriate isotypic controls. Briefly, cells were rinsed twice in PBS, permeabilized using fixation/permeabilization buffer set (eBiosciences, #00–8333-56, Paris, France) according to the manufacturer's instructions and stained with mouse anti-Prolyl 4-hydroxylase (P4H) (Abcam, #ab44971, dilution 1/100) or rabbit anti-K14 (Abcam, #ab15461, Paris, France, dilution 1/500) for 1 h, along with the appropriate isotypic controls. Cells were rinsed twice and then stained with goat anti-mouse Alexa 488 or goat anti-rabbit Alexa 488 secondary antibodies (Invitrogen, respectively #A-11029 and #A-11034, dilution 1/500 in permeabilization buffer). A minimum of 10^4 viable cell gated events were acquired on a FACScalibur flow cytometer using Cell Quest software (Becton Dickinson, Grenoble, France) and data were analyzed using WinMDI software (developed by JC Trotter).

QPCR

For the gene expression studies RNA was extracted from treated human fibroblasts and keratinocytes using the RNeasy mini kits (Qiagen, Hilden, Germany). The cDNA was prepared using the SuperScript III First-Strand Synthesis System and random hexamers (Invitrogen Corporation). Briefly, for each reaction 2 μL of diluted cDNA, 10 μL of SYBR green master mix, 0.15 μL of 10 μM forward and reverse primers and 7.7 μL of nuclease-free water was used making a total volume of 20 μL. Q-PCR was carried out using the Mx3500P Real-Time PCR system (Stratagene, NSW, Australia). The primer sequences are shown in Supplementary Table S2. The relative expression levels of KP enzyme transcripts were calculated using a mathematical model based on the individual Q-PCR primer efficiencies and the quantified values were normalized against the housekeeping gene 18 S. From these values, fold-differences in the levels of transcripts between individual untreated and treated cell cultures were calculated according to the formula $2^{-\Delta\Delta Ct}$.

HIGH PERFORMANCE LIQUID CHROMATOGRAPHY (HPLC)

TRYP, KYN, and KYNA were measured using an Agilent 1100 series HPLC system equipped with a G1329A temperature-controlled autosampler, a G1314A variable wavelength detector, a G1321A xenon flash lamp fluorescence detector, and a Zorbax 300SB C18 reversed-phase 4.6 × 250 mm column (Agilent Technologies, North Ryde, Australia) and mobile phase consisting of ammonium acetate buffer (0.1 M, pH 4.65) containing 0.02% (v/v) acetonitrile. KYN was measured by UV absorbance at 365 nm, TRYP was measured using fluorescence (Ex285 nm/Em365 nm), and KYNA was measured by fluorescence (Ex254 nm/Em404 nm) after postcolumn derivatization with zinc acetate as previously described [Kapoor et al., 1994].

GAS CHROMATOGRAPHY/MASS SPECTROMETRY (GC/MS)

Culture supernatants were assayed for QUIN as previously described [Kerr et al., 1997]. QUIN concentrations were calculated with the following formula: total concentration of QUIN (in nanomolar) detected in cell culture supernatants minus the concentration of QUIN (in nanomolar) present in the culture medium before addition to cells. Samples were similarly analyzed for PIC analysis using d4-picolinic acid as an internal standard. QUIN and PIC samples were analyzed by gas chromatography-mass spectrometry (GC-MS) with the spectrometer operating in electron capture negative ionization mode. Selected ions (m/z 273 for PIC and m/z 277 for d4-PIC) were then monitored [Smythe et al., 2002]. The limits of quantification were ± 1 fmol (injected onto the column) at signal-to-noise ratios of 10:1. Experiments were performed in triplicate using supernatants from primary fibroblast and keratinocyte cultures derived from three different human skins and. All results are expressed as the mean ± SEM.

NAD(H) MICROCYCLING ASSAY

Following 24 h incubation with 0–50 μM concentrations of KP metabolites and/or Resvertrol/MK-801, intracellular NAD^+ levels were measured spectrophotometrically using the thiazolyl blue

microcycling assay established by Bernofsky and Swan (1973) adapted for 96 well plate format by Grant and Kapoor (1998). NAD^+ levels were also measured following varying times of exposure to a UVB lamp (Stratagene 2000 illuminator specially equipped with FG15T8 bulbs). The following procedures were performed in the dark. Plates containing cells were washed twice with PBS and scraped using a cell scraper. 125 μL of the reaction mixture containing 120 mM bicine, 0.6 M ethanol, 2 mM PMS, 0.5 mM MTT, and 1 mL of ADH (20 mg in 20 mL TRIS buffer) was added to each well in a 96 well plate. Six microliter of the cell suspension was added to the well and incubated for 10 min. Total NAD^+ was calculated as the change in total NAD(H) and NADH concentrations, measured as change of absorbance at 570 nm on the BioRad 690XR microplate reader (BioRad, Hercules).

EXTRACELLULAR LDH ACTIVITY

To determine cell viability after treatment with 0–50 μM concentrations of KP metabolites and/or Resveratrol/MK-801, or exposure to a UVB lamp, cell supernatants were collected and assayed for extracellular lactate dehydrogenase (LDH) activity using a standard spectrophotometric technique described by Koh and Choi (1987). The release of LDH is associated with damage to the cell membrane and cell death, and provides an index for toxicity. Briefly, 50 μL of sodium pyruvate (11.5 mM) and 50 μL of the cell supernatant was added to each well. This was followed by the addition of 100 μL of NADH in K_2HPO_4 buffer (700 μM). LDH activity was measured kinetically at a wavelength of 340 nm using the BioRad 690XR microplate reader (BioRad, Hercules).

BRADFORD PROTEIN ASSAY FOR THE QUANTIFICATION OF TOTAL PROTEIN

A Bradford protein assay [Bradford, 1976] was carried out to adjust for TRYP, KYN, KYNA, QUIN, PIC, intracellular NAD^+ concentrations, and extracellular LDH activity using the Pierce BCA Protein Assay Kit (Thermo Scientific, Illinois, USA).

CO-CULTURE SYSTEMS OF IDO EXPRESSING FIBROBLASTS AND BYSTANDER CELLS

A 30 mm Millicell Sterilized Culture Plate Inserts (Millipore, Bedford, MA), was used to establish a co-culture system in which fetal fibroblasts were grown on the upper chamber of a six-well plate, while bystander cells including either keratinocytes, or T cells were cultured on the lower chamber. This eliminated direct contact between fibroblasts and bystander cells.

T CELL CULTURE

Total human peripheral blood mononuclear cells (PBMCs) were isolated by density gradient sedimentation using Histopaque-1077 (Sigma) according to the manufacturer's protocol. Briefly, whole blood was layered on an equal volume of Histopaque and centrifuged at 2,000 r.p.m. for 20 min at room temperature and stopped without any brake. PBMCs were isolated and resuspended in RPMI 1640 + 10% FBS and pelleted by centrifugation at 2,000 r.p.m. for 10 min and were further washed twice in PBS + 1% FBS. Using PE-conjugated mouse anti-human CD3 mAb (BD, Oakville, ON), FITC-conjugated mouse anti-human CD4 mAb (BD), and allophycocyanin (APC)—conjugated mouse anti-human CD8 mAb (BD) at the concentration of 20 μL/10^6 cells, we stained the PBMCs. The cells were then incubated at room temperature for 30 min. Thereafter, cells were washed twice and resuspended at 10^7 cells/mL in PBS + 1% FBS for fluorescent activated cell sorting (FACS). For preparation of a pure population of $CD3^+CD4^+$ and $CD3^+CD8^+$ T cells, we gated on $CD3^+CD4^+$ and $CD3^+CD8^+$ T cells after excluding the dead cells and cell debris based on FSC and SSC parameters and sorted these two cell populations into separate tubes. After being sorted from blood, T cells were propagated in RPMI 1,640 (Hyclone, UT) supplemented with 10% FBS, 0.1 U penicillin/mL, and 0.1 mg streptomycin/mL at 37°C in a humidified 5% CO_2 atmosphere to be used for further treatment.

CELL SURVIVAL EVALUATION

The survival of fetal fibroblasts and keratinocytes, and two different sensitive ($CD4^+$ and $CD8^+$ T cells) and two different resistant (dermal fibroblasts and keratinocytes) cell types exposed to UVB treated and IFN-γ were compared by 7-AAD staining. 7-AAD intercalates into double-stranded nucleic acids and penetrates cell membranes of damaged cells. After each treatment, cells were harvested, washed in PBS, stained for 7-AAD and then examined using FACS analysis, according to the manufacturer's protocol (BD).

STATISTICAL ANALYSIS

Results obtained are presented as the means ± the standard error of measurement (SEM). One-way analysis of variance (ANOVA) and post hoc Tukey's multiple comparison tests were used to determine statistical significance between treatment groups. Differences between treatment groups were considered significant if P was less than 0.05 ($P < 0.05$).

RESULTS

PURITY OF CULTURES OF HUMAN SKIN CELLS

Cultures of foetal fibroblasts and keratinocytes were immunostained with the respective markers fibronectin and cytokeratin and were 90–95% pure after 7 days in culture. After 4 weeks and repeated changing of medium, purity of the neuronal cultures reached 98–99% (Fig. 2). Further analysis using flow cytometry showed that 99.1% of fetal fibroblast cells express P4H, another marker for fibroblasts. Similarly, flow cytometry analysis demonstrated that 97.5% of fetal keratinocytes express K14, a marker for keratinocytes.

UVB INDUCED TIME DEPENDENT DECREASE IN INTRACELLULAR NAD+ AND CELL VIABILITY

A time dependent study assessing intracellular NAD^+ levels and cell viability was performed to find optimal exposure time to UVB radiation at 2 mJ/cm^2 that will cause cell damage but will not completely destroy a majority of the cells. Over the period of 30 min, a decrease in intracellular NAD^+ levels was observable in both fibroblasts and keratinocytes, although fibroblasts appear to be more susceptible to UVB induced damage than keratinocytes (Fig. 3A). Cell viability in the same study (Fig. 3B) showed corresponding results, with the fibroblasts displaying more release of extracellular LDH

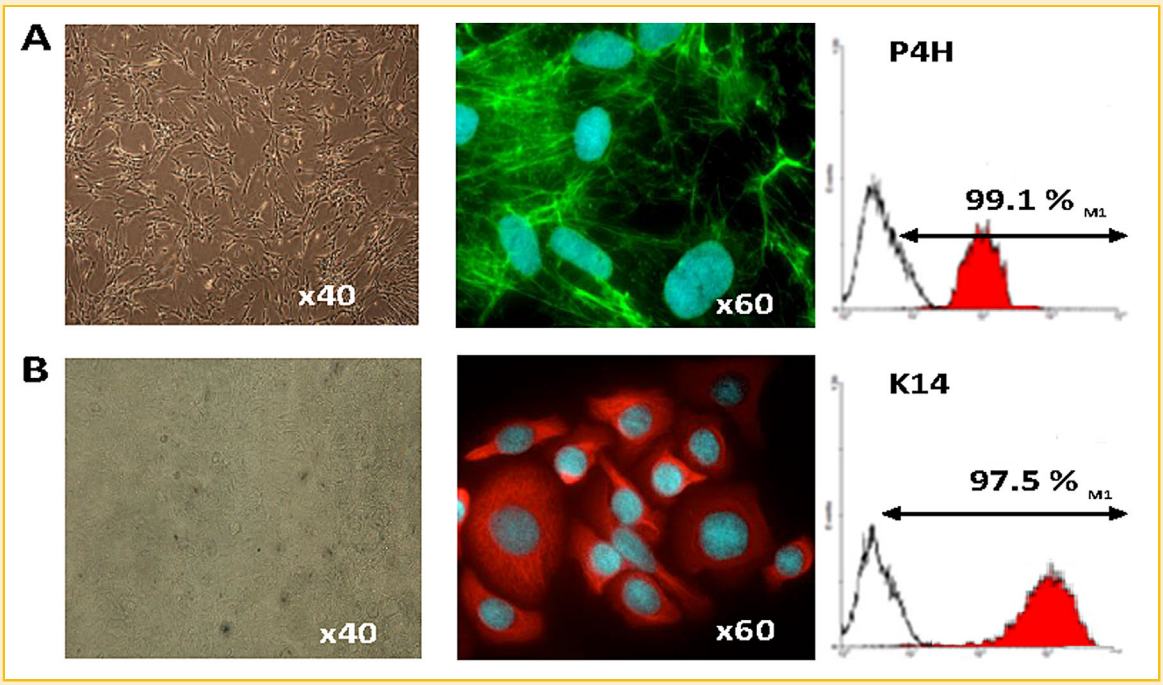

Fig. 2. Purity of human primary fibroblast and keratinocyte cell cultures. (A) Fibroblasts labelled with fibronectin and P4H, and (B) Keratinocytes labelled with cytokeratin and K14. Full histograms represent test samples, solid lines represent isotypic controls.

than keratinocytes over the course of a 30-min timed UVB exposure. Our data indicates that 50% cellular damage occurred after 10 min of exposure to UVB, and was used as the duration of UVB exposure in subsequent experiments. ($n = 3$ for each treatment group).

EXPRESSION OF KP ENZYMES IN HUMAN FOETAL FIBROBLASTS AND KERATINOCYTES

Primer sets were developed and validated to identify mRNA transcripts for indoleamine 2,3 dioxygenase I (IDO1), indoleamine 2,3 dioxygenase II (IDO2), tryptophan 2,3 dioxygenase (TDO2), kynureninase (KYNU), kynurenine aminotransferase I (KAT I), kynurenine aminotransferase II (KAT II), kynurenine aminotransferase III (KAT III), monoamine oxidase A (MAOA), monoamine oxidase B (MAOB), kynurenine 3-hydroxylase (KMO), aspartate aminotransferase (GOT2), quinolinic acid phosphoribosyl transferase (QPRT), 3-hydroxyanthranilate 3,4-dioxygenase (3-HAA), tryptophan hydroxylase I (TPH I), tryptophan hydroxylase II (THP II), arylformamidase (AFMID), aminocarboxymuconate semialdehyde decarboxylase (ACMSD), nicotinamide mononucleotide adenyl transferase I (NMNAT-I), nicotinamide mononucleotide adenyl transferase II (NMNAT-II), nicotinamide mononucleotide adenyl transferase III (NMNAT-III), nicotinic acid phosphoribosyl transferase (NAPT), and nicotinamide phosphoribosyl transferase (NMPT). All of the investigated transcripts were found to be expressed in human foetal fibroblasts and keratinocytes, however in highly variable levels (Fig. 4). IFN- γ (100 IU/L) and/or UVB radiation was applied at a rate of 2 mJ/cm^2 for 10 min to induce KP enzymes and all enzymes were analyzed 24 h after application of IFN-γ and/or UVB treatments as indicated by time course studies [Guillemin et al., 2007] ($n = 3$ for each treatment group).

Transcripts encoding IDO1 were expressed at $>10^2$–fold of untreated fibroblast cells for all three treatments. Transcripts encoding IDO2 were significantly down regulated by UVB radiation and combination of UVB and IFN-γ ($>10^{-1}$–fold) although IFN-γ by itself showed no significant changes. KYNU levels showed small but significant increases by IFN-γ and UVB alone (3.2 fold and 4.1 fold respectively) but in combination, levels of transcripts increased by 9 fold. The kynureninase amino transferases (KAT I, KAT II, and KAT III) did not display significant variance in response to UVB treatment or cytokine treatment. A number of other transcripts also showed no significant change in the levels of transcripts expressed in response to IFN-γ and/or UVB, including: TDO2, MAOA, MAOB, NMNAT-I, TPH I, and TPH II. KMO transcripts in fibroblasts showed up regulation (3.6, 5.2, and 6.4 fold increased respectively). GOT2 showed a 6.5 fold increase in expression with the cytokine and UVB treatment combined, and no significant change with either treatment alone. Levels of transcripts encoding QPRT showed no significant change in response to IFN-γ alone, however small but significant down regulation was observed in response to UVB and the combination of treatments (0.3 and 0.2 fold of control respectively). 3-HAO displayed up regulation of transcripts across all three treatments (5.2, 6.3, and 6.9 fold respectively). AFMID displayed large increases in transcripts (>50 fold) across all three treatments. Transcripts encoding ACMSD were up regulated by 4 fold in response to IFN- γ but no significant change was show in other treatments. NMNAT-II transcripts increased by four fold, 4.7 fold and 6.8 fold

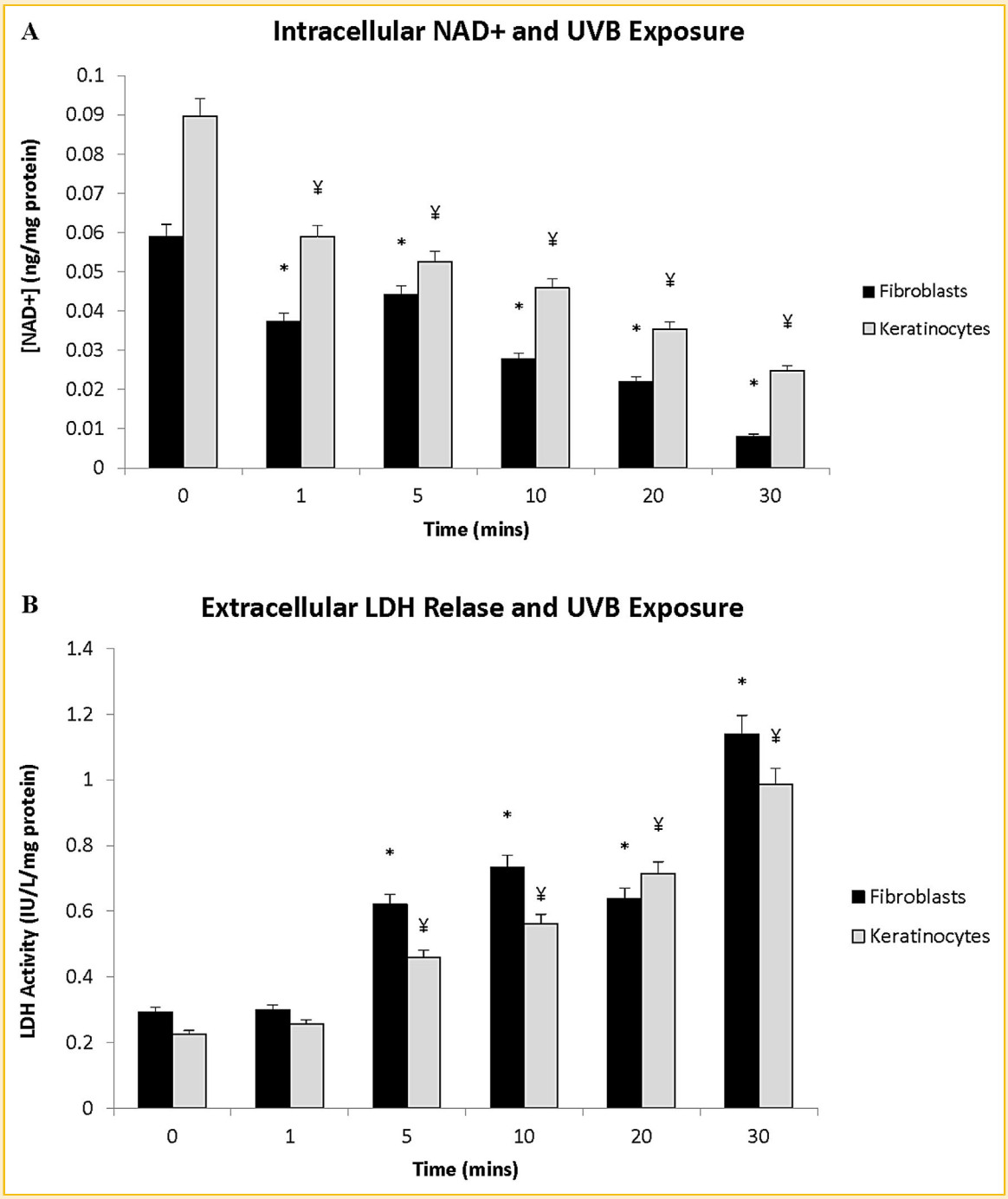

Fig. 3. The effect of UVB radiation (2 mJ/cm^2) on (A) intracellular NAD$^+$ levels and (B) extracellular LDH activity in human foetal fibroblasts and keratinocytes over 30 min. *$P < 0.05$ compared to control in human foetal fibroblasts. ¥ $P < 0.05$ compared to control in human foetal keratinocytes. ($n = 3$ for each treatment group).

respectively for each of the three treatments. Transcripts encoding NMNAT-III displayed significant up regulation in response to IFN-γ (77.7 fold) UV and UV and IFN-γ ($>10^3$ fold of control). No significant differences were observed in the expression of NMNAT-I. Similarly, NAPT displayed levels of transcripts $>10^4$ fold of control in all three treatment cases. An increase of $\sim 10^2$ was observed in response to IFN-γ treatment and UVB + IFN-γ treatment, although UVB treatment by itself showed only a 6.7 fold increase of transcripts compared to untreated cells.

Similarly, transcripts encoding IDO1 were expressed at $>10^2$ fold of untreated keratinocyte cells for all three treatments. Transcripts encoding IDO2 were significantly down regulated by UVB radiation and combination of UVB and IFN-γ ($>10^{-1}$–fold), although IFN-γ by itself showed no significant changes. KYNU levels were not

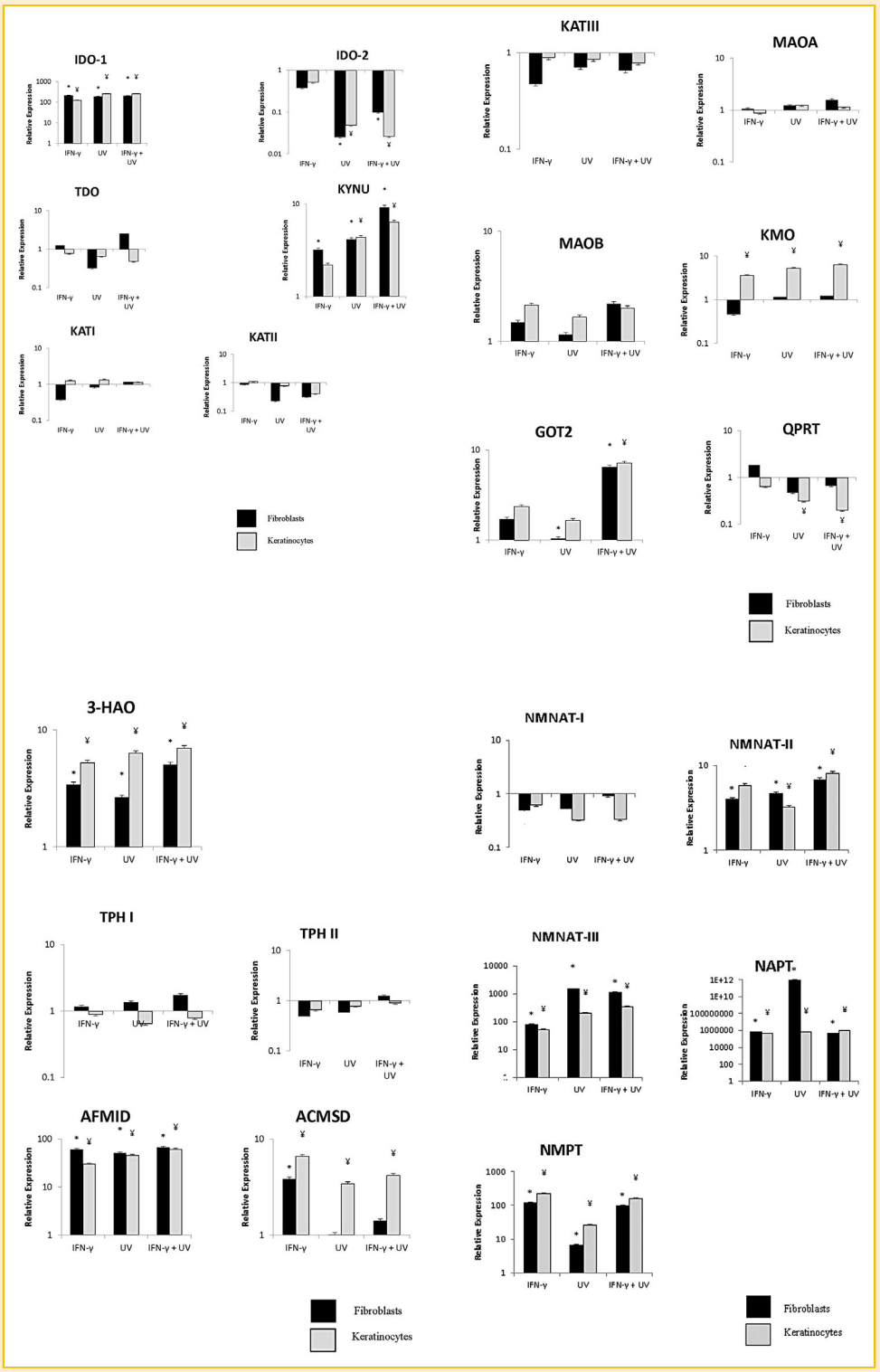

Fig. 4. Relative levels of transcripts encoding enzymes in the KP (IDO-1, IDO-2, TDO, KYNU, KAT I, KAT II, KAT III, MAOA, MAOB, KMO, HOT2, QPRT, 3-HAA, THP1, THP2, HPRT, AFMID, ACMSD, NMNAT-1, NMNAT-2, NMNAT-3, NAPT, and NMPT) following treatment with IFN-γ (100 U/mL), UVB radiation (2 mJ/cm^2) or the combination of these two treatments. Levels of all transcripts are normalized to levels observed in untreated control cells (base-line) and expressed in a logarithmic scale. *$P < 0.05$ compared to control in human foetal fibroblasts. ¥ $P < 0.05$ compared to control in human foetal keratinocytes. ($n = 3$ for each treatment group).

significantly affected by IFN-γ alone (2.2 fold increase); however, UVB and the combination of treatments increased transcripts increased by 4.4 and 6.4 fold respectively. TDO2, KAT I, KAT II, KAT III, MAOA, MAOB, TPH I, TPH II, and NMNATI all remained very close to basal levels and transcripts were not altered significantly by the different treatments. KMO and GOT2 both showed some increase in transcripts, mainly in response to the combination of UVB and IFN-γ with levels of transcripts expressed at 6.4 and 7.2 times control. Levels of QPRT transcripts were all lower than control in keratinocytes; however, IFN-γ by itself made no significant change. 3-HAO showed increased transcript levels in response to all treatments, and showed the greatest increase with the combination of UVB and IFN-γ (7 fold increase). AFMID showed marked transcriptional up regulation with levels expressed at 30 fold, 46 fold, and 61 fold respectively in response to IFN-γ, UVB and the combination of the two treatments. ACMSD showed small transcriptional up regulations (6.6 fold, 3.4 fold, and 4.2 fold respectively). NMNAT-II transcripts were up regulated between 3–8 fold across the treatments, and NMNAT-III showed a >50 fold increase in response to IFN-γ and a $>10^2$ fold increase in response to UVB and IFN-γ + UVB. As in fibroblasts, NAPT showed the greatest transcriptional up regulation in response to each treatment ($>10^3$ fold). Lastly, NMPT transcripts were up regulated significantly in response to treatments involving IFN-γ ($>10^2$) whereas UVB alone increased transcripts by 26 fold control levels.

IMMUNOCYTOCHEMICAL DETECTION OF KP COMPONENTS IN FIBROBLASTS AND KERATINOCYTES

Immunocytochemical detection of KP enzymes are in general agreement with the real time PCR results (Fig. 5). For both primary fibroblasts and keratinocytes, immunostaining for IDO-1, TDO, KMO, KYNU, KAT-II, and QPRT, NMNAT-II and NMNAT-III was perinuclear and cytoplasmic. In both cell types, NMNAT-I labelling was mainly detected in the nucleus. In fibroblasts and keratinocytes, QUIN immunostaining was located in the cytoplasm. Finally, for fibroblasts and keratinocytes, staining for the structural protein fibronectin and cytokeratin indicated localization throughout the cytoplasm respectively.

HPLC QUANTIFICATION OF TRYP, KYN, AND KYNA IN FIBROBLASTS AND KERATINOCYTES

Fibroblasts and keratinocytes were treated with IFN-γ and or UVB radiation and allowed to incubate for 24 h at 37°C before HPLC analysis. 100 IU/L IFN-γ was used and UVB radiation was applied at 2 mJ/cm^2 for 10 min. Concentrations were calculated as a change in the levels of the metabolite being analyzed from levels present in control (untreated) cells. $n = 3$ for all treatment groups and a P-value of less than 0.05 was regarded as statistically significant ($P < 0.05$). In both fibroblasts and keratinocytes exposed to UVB and/or IFN-γ, TRYP levels were significantly reduced compared to non-treated groups, (Fig. 6A). A difference to note is the varied levels of TRYP in control treatment groups. Fibroblast TRYP levels were very low in the control group (2.4 ± 0.13 μM) as opposed to the keratinocytes group (54.4 ± 2.9 μM).

Fibroblasts and keratinocytes treated with UVB and/or IFN-γ showed a small but significant increase in KYN production (Fig. 6B). In fibroblasts, KYN was present in the control group at a concentration of 0.24 ± 0.013 μM, and treatment with UVB and IFN-γ together showed the largest increase from control 2.86 ± 0.15 μM. Basal levels of KYN in keratinocytes were present at 0.51 ± 0.027 μM, and production of KYN significantly increased when treated with UVB (0.65 ± 0.034 μM) or IFN- γ alone (0.92 ± 0.049 μM), and in combination.

Changes in concentrations of KYNA occurred across both fibroblasts and keratinocytes in all three-treatment groups. Untreated fibroblasts produced KYNA at a concentration of 3.70 ± 0.20 μM). Fibroblasts treated with IFN-γ displayed decreases in KYNA concentrations (2.85 ± 0.15 μM). UVB and UVB + IFN-γ together produced an increase of KYNA levels (4.44 ± 0.24 μM and 5.9 ± 0.32 μM respectively). Concentration of KYNA in untreated keratinocytes (Fig. 6C) was 2.7 ± 0.13 μM and increases in concentration were recorded across all three treatments at 3.35 ± 0.16 μM, 4.83 ± 0.24 μM, and 3.97 ± 0.20 μM respectively.

GC/MS QUANTIFICATION OF PIC AND QUIN IN FIBROBLASTS AND KERATINOCYTES

Fibroblasts and keratinocytes were treated with IFN-γ and/or UVB radiation and allowed to incubate for 24 h at 37°C before HPLC analysis. 100 IU/L IFN-γ was used and UVB radiation was applied at a rate of 2 mJ/cm^2 for 10 min. Concentrations were calculated as a change in the levels of the metabolite being analysed from levels present in control (untreated) cells. $n = 3$ for all treatment groups and a P-value of less than 0.05 was regarded as statistically significant ($P < 0.05$).

Concentrations of PIC in fibroblast cells decreased with subsequent treatments (Fig. 7A). Untreated cells produced PIC at a concentration of 1.16 ± 0.06 μM. UVB radiation decreased the concentration to 0.85 ± 0.04 μM, while IFN-γ decreased levels to 0.43 ± 0.24 μM. The combination of the two treatments showed a great decrease in PIC levels, at a concentration of 0.22 ± 0.01 μM. UVB and IFN-γ treatments alone did not affect PIC concentrations in keratinocytes significantly. The combination of the treatments increased levels of PIC from 0.41 ± 0.19 μM in control to 0.59 ± 0.32 μM, although this did not reach statistical significance.

QUIN concentrations increased significantly with the three treatments (Fig. 7B) in human keratinocytes but not in fibroblasts. Untreated keratinocytes produced QUIN at a concentration of 0.143 ± 0.07 μM. UVB radiation increased concentrations to 0.171 ± 0.08 μM. IFN-γ also increased the levels of QUIN to 0.180 ± 0.09 μM and the combination of the two treatments reached a concentration of 0.178 ± 0.07 μM. QUIN concentrations in fibroblasts following UVB and IFN-γ treatments alone remained unchanged.

EFFECT OF KP METABOLITES ON INTRACELLULAR NAD+ LEVELS AND CELL VIABILITY IN FIBROBLASTS AND KERATINOCYTES

A summary of the effect of treatment with KP metabolites on intracellular NAD^+ levels and cell viability in fibroblasts and keratinocytes is shown in Table I. Application of TRYP (Fig. 8A) increased NAD^+ levels in fibroblasts and keratinocytes in a dose dependent manner. KYN (Fig. 8B) showed dose dependent decrease

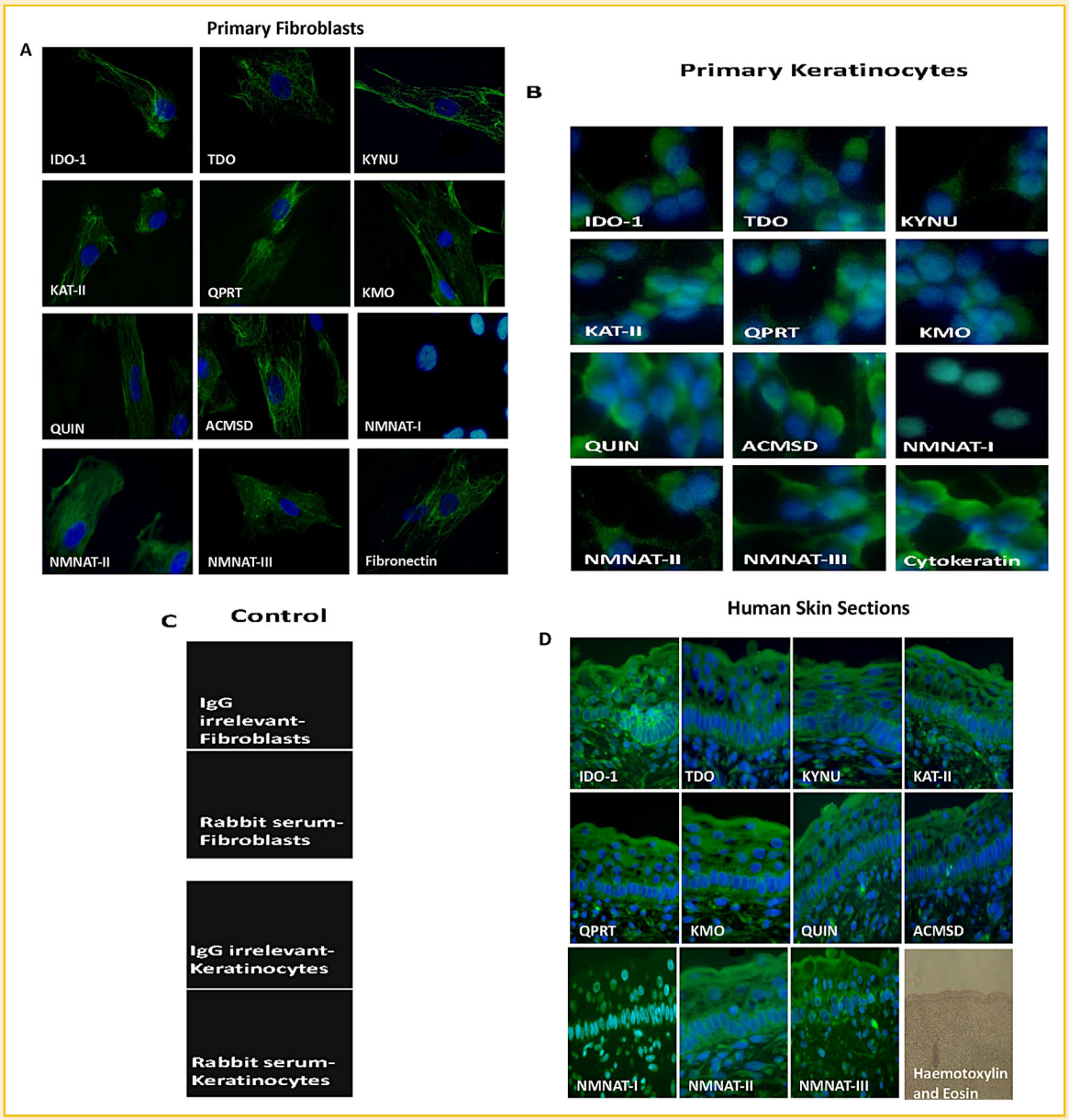

Fig. 5. Immunodetection of kynurenine pathway enzymes and products in human neurons and brain. (A) Cultures of human primary fibroblasts were immunostained for the enzymes IDO-1, TDO, KYNU, KAT-II, KMO, QPRT, ACMSD, NMNAT-I, NMNAT-II, NMNAT-III, as well as for QUIN and fibronectin as indicated. (B) Cultures of human primary keratinocytes were immunostained for the enzymes IDO-1, TDO, KYNU, KAT-II, KMO, QPRT, ACMSD, NMNAT-I, NMNAT-II, NMNAT-III, as well as for QUIN and cytokeratin as indicated. (C) Control preparations of cultures of human primary neurons: irrelevant IgG and nonimmune rabbit serum staining of human primary fibroblasts and keratinocytes. (D) Human skin sections were also immunostained for IDO-1, TDO, KYNU, KAT-II, KMO, QPRT, ACMSD, NMNAT-I, NMNAT-II, NMNAT-III, haematoxylin, and eosin staining as indicated.

in NAD^+ in keratinocytes at concentrations exceeding 10 μM, and a dose dependent decrease in fibroblasts at concentrations above 0.1 μM. Treatment with KYNA (Fig. 8C) showed no significant difference in NAD^+ levels in fibroblasts and keratinocytes. AA (Fig. 8D) and 3-HAA (Fig. 8F) both produced a dose dependent decrease in NAD^+ levels in keratinocytes and in fibroblasts. 3-HK (Fig. 8E) showed a significant decline in NAD^+ levels at concentrations greater than 1 μM in fibroblasts and 10 μM in keratinocytes. PIC (Fig. 8H) reduced NAD^+ levels in fibroblasts at concentrations greater than 1 μM whereas NAD^+ levels declined in keratinocytes at concentrations greater than 0.5 μM. QUIN (Fig. 8G) showed an increase in NAD^+ at 0.5 μM, and then decreased with subsequent dosages in fibroblasts. QUIN increased NAD^+ in keratinocytes up to 10 μM but declined at higher concentrations.

Consistent with the results obtained for intracellular NAD^+ levels, no significant change was observed in extracellular LDH activity for both fibroblasts and keratinocyte cultures treated with TRYP (Fig. 9A) or KYNA up to 50 μM (Fig. 9C). However, treatment with

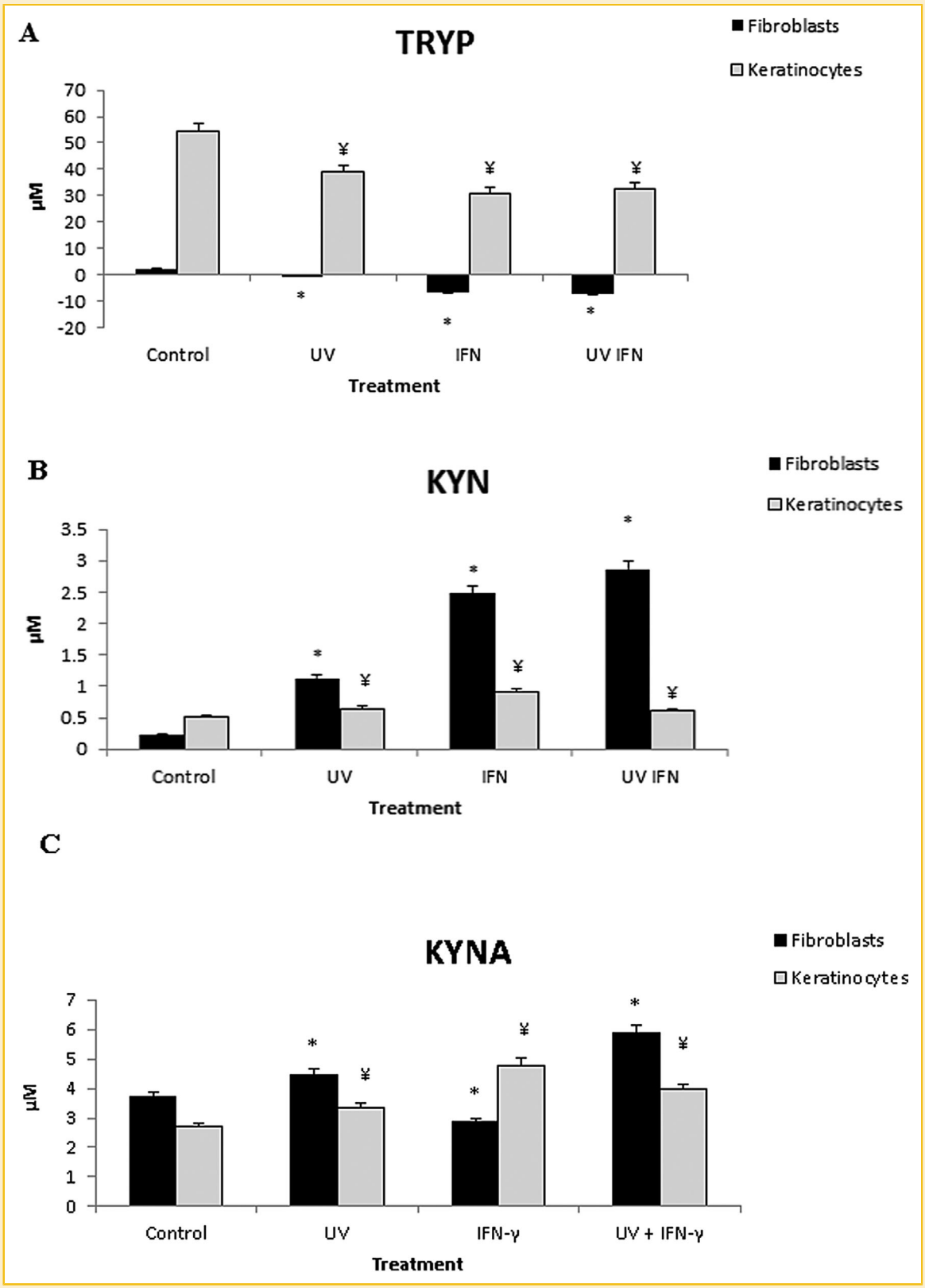

Fig. 6. The effect of UVB radiation (2 mJ/cm^2 for 10 min), IFN-γ administration (100 IU/mL) and the combination of these both on the production of (A) TRYP, (B) KYN, and (C) KYNA by human foetal fibroblasts and keratinocytes following 24 h incubation. *$P < 0.05$ compared to control in human foetal fibroblasts. ¥ $P < 0.05$ compared to control in human foetal keratinocytes. (n = 3 for each treatment group).

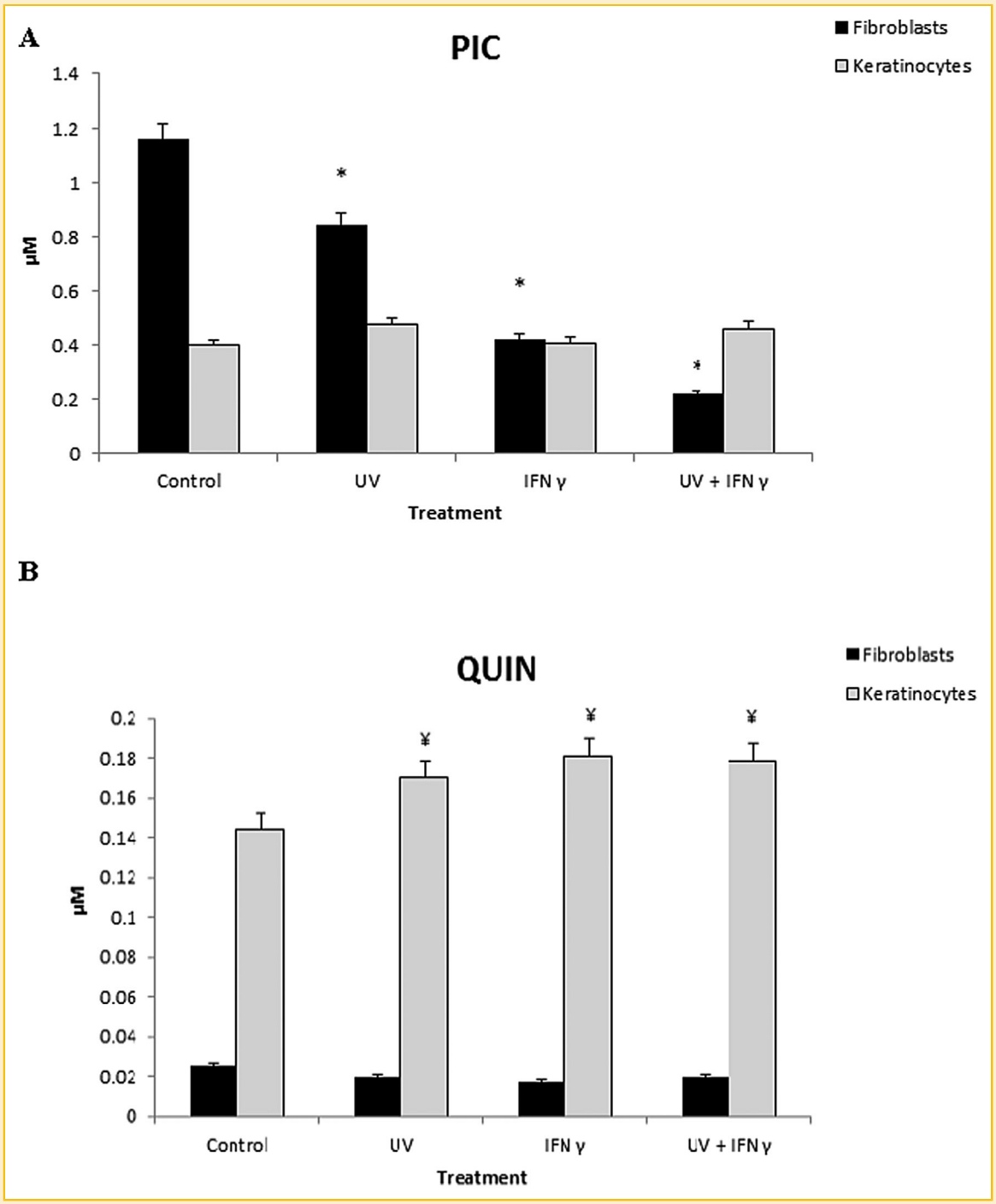

Fig. 7. The effect of UVB radiation (2 mJ/cm^2 for 10 minutes), IFN–γ administration (100 IU/mL) and the combination of these both on the production of PIC (A) and QUIN (B) by human foetal fibroblasts and keratinocytes following 24 hour incubation. * $p < 0.05$ compared to control in human foetal fibroblasts. ¥ $p < 0.05$ compared to control in human foetal keratinocytes. ($n = 3$ for each treatment group)

KYN (Fig. 9B) increased extracellular LDH activity at concentrations above 0.1 μM in fibroblasts and 10 μM in keratinocytes. A dose-dependent increase in extracellular LDH activity was observed in fibroblasts and keratinocytes treated with AA (Fig. 9D) and 3-HAA (Fig. 9F) at concentrations above 0.1 μM and 0.5 μM respectively. LDH activity was also increased for cells treated with 3-HK at concentrations above 1 μM in fibroblasts and 10 μM in keratinocytes (Fig. 9E). PIC (Fig. 9G) increased LDH activity at concentrations greater than 1 μM in fibroblasts and 0.5 μM in keratinocytes. QUIN (Fig. 9H) showed an increase in LDH activity in a dose dependent manner at concentrations greater than 0.5 μM in fibroblasts and 10 μM in keratinocytes.

TABLE I. Summary of the Effects of KP Metabolites on Cell Viability and NAD+ Production in Human Foetal Fibroblasts and Keratinocytes

	LDH Release		NAD^+ Levels	
Metabolite	Fibroblasts	Keratinocytes	Fibroblasts	Keratinocytes
TRYP	↓	↓	–	↑
KYN	↑	↑	↓	↑
KYNA	↑	↑	↓	↓
AA	↑	↑	↓	↓
3-HK	↑	–	–	↑
3-HAA	↑	↑	↓	↓
PIC	↑	↑	↑	↓
QUIN	↑	↓	↑	↑

↑denotes an increase in extracellular LDH release or intracellular NAD^+ levels. ↓denotes a decrease in extracellular LDH release or intracellular NAD^+ levels. – denotes no significant ($p < 0.05$) change in LDH and NAD^+ levels.

EFFECT OF UVB AND IFN-Γ TREATMENT ON CELL SURVIVAL RATE OF HUMAN SKIN CELLS AND T CELLS

As the viability of skin cells can have a profound effect on immune tolerance, it is vital to determine whether UVB and IFN-γ can also differentially influence the viability of skin and immune cells. Therefore, we cultured fibroblasts and keratinocytes were treated with UVB, IFN-γ, or UVB and IFN-γ, and co-cultured with $CD4^+$ and $CD8^+$ T cells respectively. After day 4, bystander cells were collected and their survival rates were determined using 7-AAD staining staining with flow cytometry. As demonstrated in Figure. 10, no significant differences were observed in cells co-cultured with non-treated fibroblasts. Treatment with IFN- γ significantly reduced survival rates for $CD4^+$ (21%) and $CD8^+$ T cell (18%) but not fibroblast and keratinocytes. A more profound decline in survival rates were observed for fibroblast (68%), keratinocyte (51%), $CD4^+$ (41%) and $CD8^+$ T cell (48%) following treatment with UVB. A further reduction in survival rates was observed following co-treatment with UVB and IFN-γ for fibroblast (81%), keratinocyte (71%), $CD4^+$ (63%) and $CD8^+$ T cell (65%).

DISCUSSION

CHARACTERISATION OF THE KYNURENINE PATHWAY IN SKIN CELLS

In this study, we showed for the first time, that TRYP catabolism is increased in human fibroblast and keratinocyte cultures in response to IFN-γ and UVB treatment. Increased expression of IDO1 may play a protective role in skin pathology. For instance, animal wounds that have been engrafted with IDO1-expressing skin show higher expression levels of matrix metalloproteinase-1 (MMP-1). MMP-1 belongs to a family of zinc-dependent and neutral endopeptidases that serve an important role in tissue remodelling through degradation of extracellular matrix (ECM) components. Increased MMP-1 expression attenuates inflammation and improves scarring compared with controls [Fourozandeh et al., 2010]. IDO1 catabolised L-TRYP into KYN. KYN is secreted from IDO-expressing skin grafts and can affect the ECM, although the exact mechanism remains unclear. Li et al. (2014) recently showed that KYN significantly increases the expression of MMP-1 and MMP-3, whilst decreasing the expression of collagen in cultured dermal fibroblasts. The effects of KYN on MMP expression are thought to be due to activation of MEK (mitogen-activated protein kinase (MAPK)/extracellular signal-regulated kinase (ERK) kinase)-ERK1/2 MAPK signalling pathway. Furthermore, treatment with KYN at physiological levels significantly improved scarring due to fibrotic wounds in the rabbit ear [Li et al., 2014].

Besides IDO1, we have shown that UVB can also alter the expression of several other KP enzyme transcripts. As observed in previous studies [Thomas and Stocker, 1999; Guillemin et al., 2001, 2004, 2007], IDO-1 is likely to be the major determinant of this response. Our results showed that with IFN-γ and/or UVB stimulation, mRNA levels of IDO2 are decreased and are expressed in levels, which are inversely proportional to IDO1. The IDO2 gene has been shown to be homologous to IDO1, and known to have immunomodulatory properties [Ball et al., 2007; Metz et al., 2007; Yuasa et al., 2007; Lob et al., 2009]. As well, Sorensen et al. (2011) reported that IDO2 specific T-cells are cytotoxic effector cells which have the ability to both recognize and kill tumours. The ability to selectively target IDO2 and its involvement in tumour progression and immune modulation implies that IDO2 may represent a potential target for skin cancer pathogenesis and UVB-mediated skin damage. However, research into the functional roles of IDO2 in skin physiology is very new, and additional studies are needed in this area to fully understand the functionality of IDO2 in human skin cells.

The KAT enzymes (KAT I/II/III) are responsible for the production of the neuroprotective metabolite, KYNA [Okuno and Kido, 1991; Yu et al., 2006]. KYNA has been shown to antagonise the neurotoxic effects of the end KP metabolite, QUIN [Hilmas et al., 2001], by binding to the NMDA receptor glycine co-agonist site [Perkins and Stone, 1982; Kapoor et al., 1994; Jhamandas et al., 2000]. Previous reports by Asp et al. (2011) showed significant increases in the levels of KYNA in response to IFN-γ in human adult fibroblasts. However, their study did not look at the levels of KYNA in response to UVB irradiation. Our study is the first to sh;1;ow that human skin fibroblasts and keratinocytes can release KYNA in response to IFN-γ and UVB treatment, indicating that transcriptional changes in response to inflammatory cytokines and UVB are present in these cells.

As well, no significant changes were found in the mRNA expression of all three KAT enzymes across the different treatments. A previous study by Asp et al. (2011) confirmed our findings that KAT enzymes show no significant change with IFN-γ stimulation in fibroblasts, but likewise they reported marked increases in KYNA levels following cytokine treatment. However, increased mRNA expression of aspartate aminotransferase (GOT2), also known as KAT4 or mitochondrial aspartate aminotransferase (ASAT)

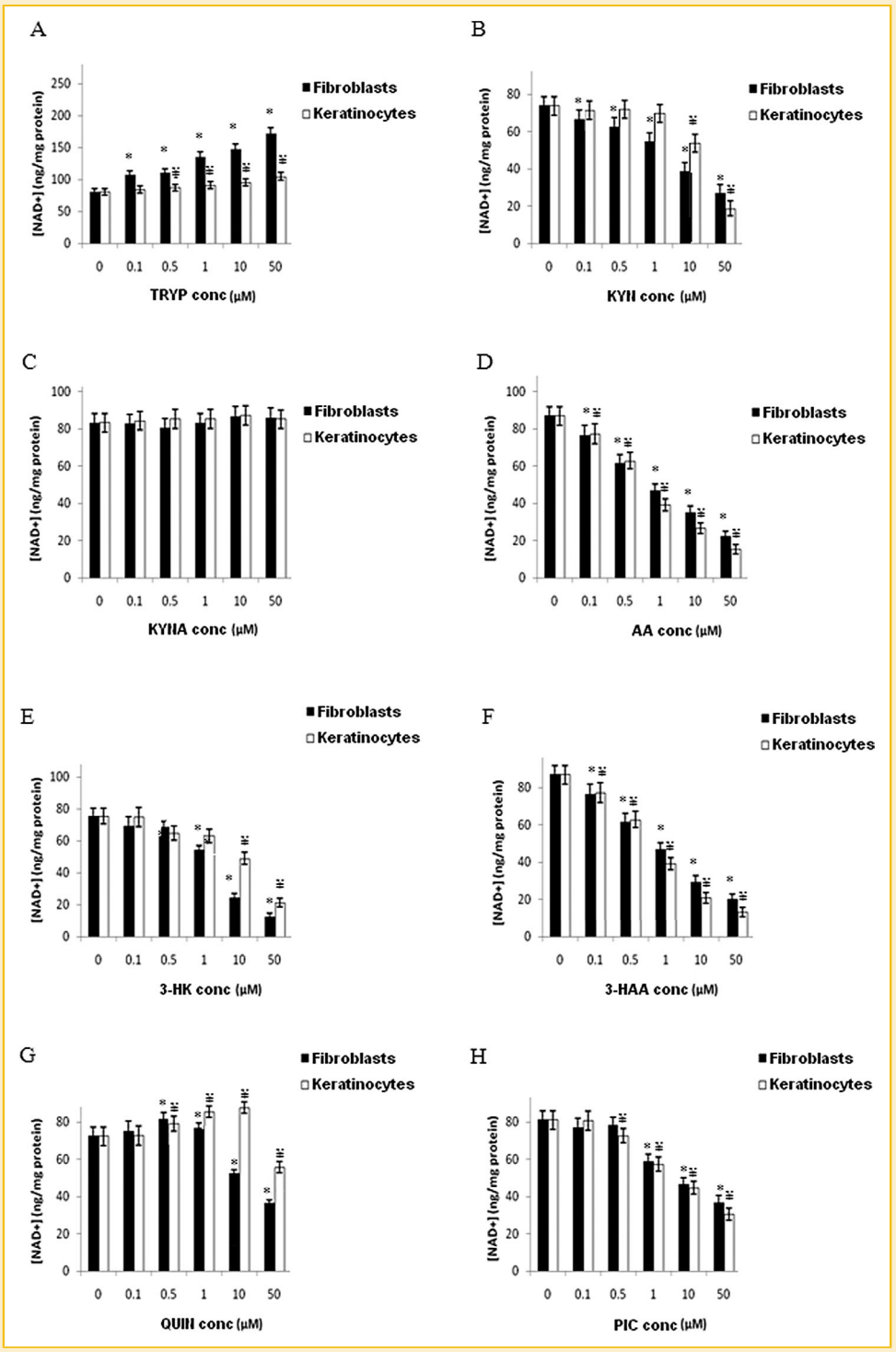

Fig. 8. The effect of TRYP (A), KYN (B), KYNA (C), AA (D), 3-HK (E), 3-HAA (F), PIC (G), and QUIN (H) (0–50 μM) on intracellular NAD^+ levels in human foetal fibroblasts and keratinocytes following 24 h incubation. *$P < 0.05$ compared to control in human foetal fibroblasts. ¥ $P < 0.05$ compared to control in human foetal keratinocytes. ($n = 3$ for each treatment group).

following UVB and IFN-γ treatment may account for the observed increase in KYNA in fibroblasts and keratinocytes. This is only the second study to look at the KP in skin cells and so definitive conclusions about these conflicting results cannot be made. Further investigation into the mechanism of regulation of KAT enzymes in human skin should be made, as the product of their enzymatic activity, KYNA has already been shown to play a major role in the pathogenesis of KP involved disorders in other human cells.

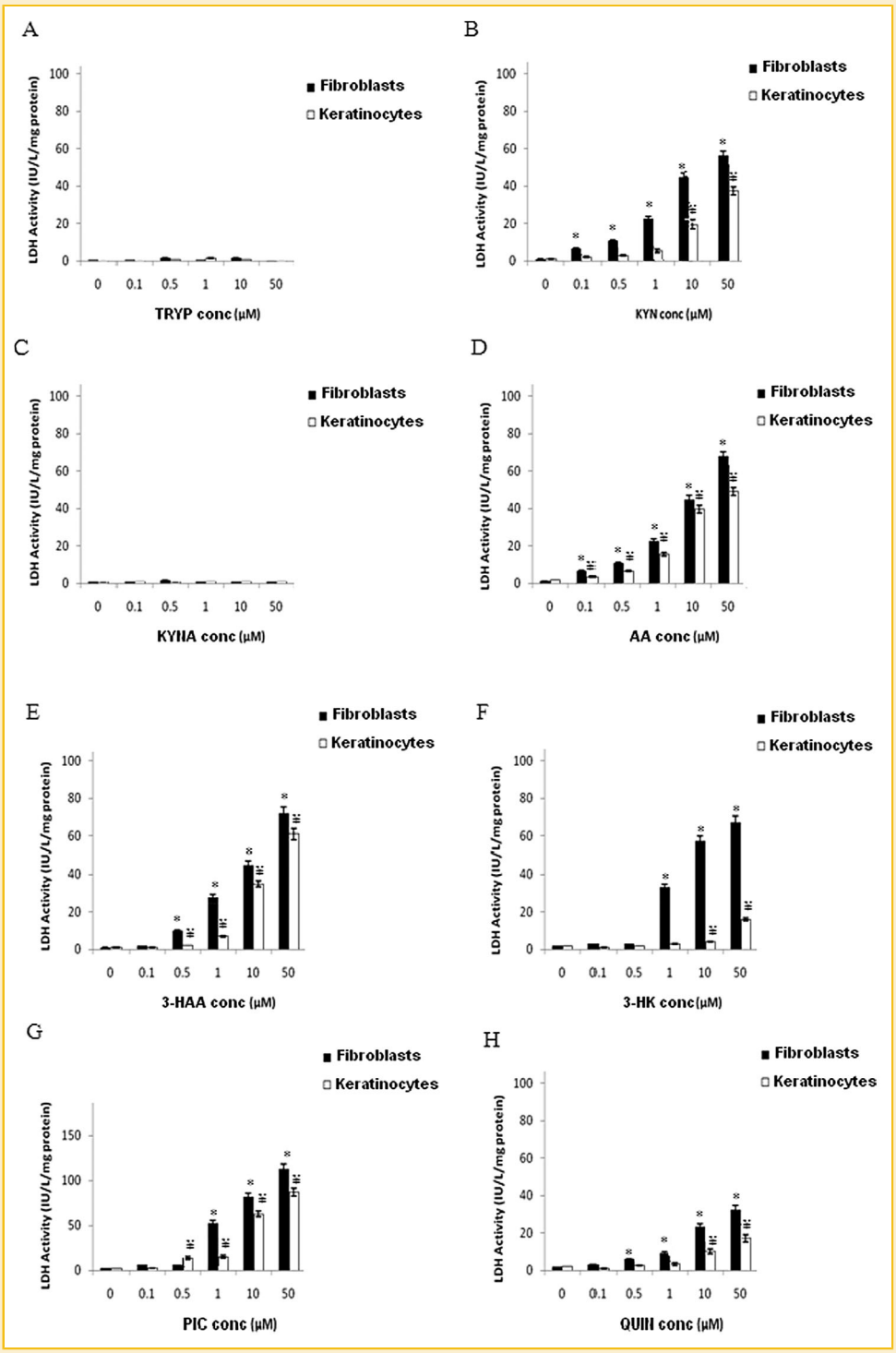

Fig. 9. The effect of TRYP (A), KYN (B), KYNA (C), AA (D), 3-HK (E), 3-HAA (F), PIC (G), and QUIN (H) on extracellular LDH levels in human foetal fibroblasts and keratinocytes following 24 h incubation. *$P < 0.05$ compared to control in human foetal fibroblasts. ¥ $P < 0.05$ compared to control in human foetal keratinocytes. (n = 3 for each treatment group).

Our study further shows that QUIN is released at significantly higher than basal levels in in response to IFN-γ and UVB treatment only in human keratinocytes, but still in a physiological range [Chen and Guillemin, 2009]. QUIN is an important excitotoxin that has been shown to induce toxicity in cells in the CNS and the periphery due to excessive activation of the NMDA receptor (reviewed by Stone and Darlington, 2002; Guillemin, 2012). Both keratinocytes and fibroblasts in the skin contain glutaminergic receptors and

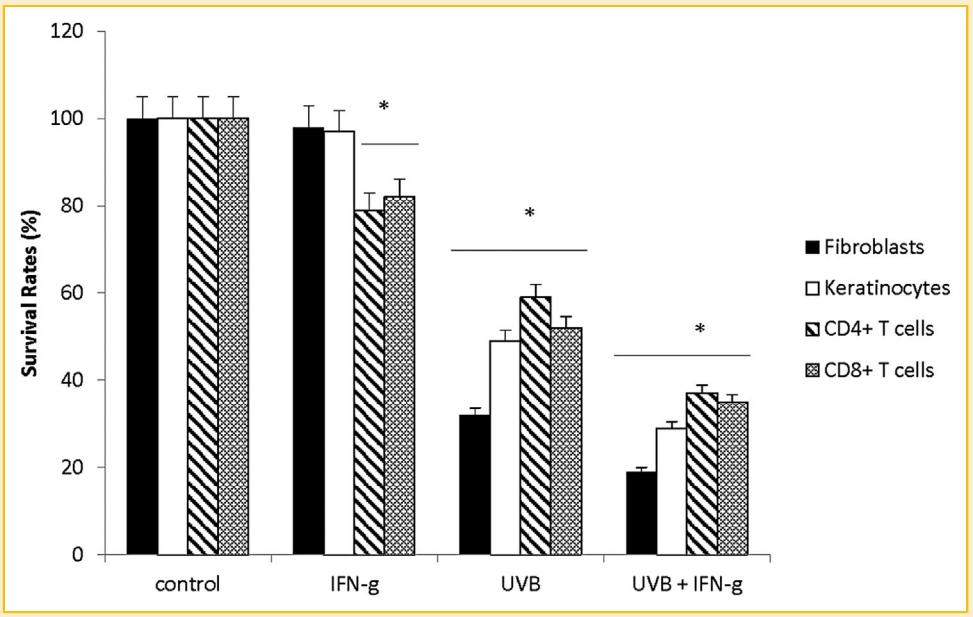

Fig. 10. Effect of UVB and IFN-γ treatment on cell survival rate of human skin cells and T cells. The results are shown for fibroblasts (solid bars), keratinocytes (open bars), purified $CD4^+$ T cells (hatched bars), and purified $CD8^+$ T cells (checked board bars). *$P < 0.05$ compared to untreated cells.

glutamate transporters [Scott et al., 2002; Nahm et al., 2004]. It is likely that chronic UV-mediated inflammation and cytokine release can stimulate QUIN-mediated activation of the NMDA receptor leading to extensive cellular degeneration. The blockade of these receptors may reduce the levels of QUIN and play an important role in skin development and regeneration following repeated inflammatory insult.

Altered KP metabolism and increased QUIN levels have been previously associated with the development of cutaneous sclerosis, resembling that seen in subcutaneous morphea, a feature of eosinophilic fasciitis [Noakes and Mellick, 2013]. Morphea is also associated with neurological findings and impairments in nerve conduction have been previously reported [Lee et al., 2002; Zulian et al., 2005]. Therefore, the concentrations of KP metabolites may play a critical role in several disease states not restricted to the CNS, as the KP represents a physiological metabolic pathway, and alterations in physiological concentrations should be seen as pathological in any system. Manipulation of the KP has been shown to produce clinical improvements. For example, Tranilast, an analogue of 3 hydroxyanthranilic acid has reported benefits in anecdotal reports and is currently still marketed in Japan for the treatment of keloid scars [Taniguchi et al., 1994].

Although significant up-regulation of KMO (the enzyme that converts KYN to 3-HK) has been shown in other studies in monocytes [Heyes et al., 1989,1992,2001], recent work by Asp et al. (2011) confirms our results which show cytokine treatment and/or UVB treatment in fibroblasts and keratinocytes has a limited effect on the expression of the KMO transcript. 3-HK has been shown to cause potent neurological damage through oxidative stress [Okudo et al., 1998], and can potentiate the neurotoxic effects of QUIN, although these two metabolites are thought to work in different ways to cause neuronal damage [Chiarugi et al., 2001]. As well as possessing neurotoxic properties, 3-HK and KYN are important protective UV filters in the human eye and are synthesized in the eye from TRYP. Stable concentrations of these metabolites in the eye are vital for prevention of cataracts [Tsentalovich et al., 2011].

Transcripts encoding TPH I/II and MAOA did not show any significant differences, and suggests that cytokine treatment and UVB radiation both seem to preferably induce IDO-1 rather than produce 5-HT and 5-HAA in human foetal fibroblasts and keratinocytes. An increase in the transcript encoding KYNU following IFN-γ and/or UVB, suggests that UVB radiation and/or inflammatory cytokine release is likely to increase the levels of downstream metabolites and induce toxicity [Guillemin et al., 2001].

PIC is an endogenous metal chelator [Jhamandas et al., 1990] which can block the toxicity of QUIN without affecting its excitatory effects. This mechanism has not yet been elucidated, but it is known that PIC does not compete for the NMDA glutamate-binding site. As well as decreasing the effects of QUIN, PIC plays various roles in immune maintenance through release of chemokines [Bosco et al., 2000], and through stimulation of antimicrobial, anti-tumoral [Leuthauser et al., 1982] and anti-viral [Fernandez and Johnson, 1977] factors. Our study shows that IFN-γ and UVB radiation both slightly potentiate levels of ACMSD expression in keratinocytes but not in fibroblasts which was induced by IFN-γ alone. However, our GC/MS analysis reported a decrease in PIC levels in response to UVB and IFN-γ treatments in fibroblasts alone. Our data suggests that the KP may be preferentially diverted towards NAD^+ production to replace depleted energy levels during periods of acute and chronic exposure to UVB radiation in fibroblasts [Jacobson et al., 2001].

Quinolinic acid phosphoribosyl transferase (QPRT) catalyses the breakdown of QUIN to the NAD^+ precursor, nicotinamide mononucleotide (NMN) and subsequently to NAD+ by nicotinamide mononucleotide adenyl transferase (NMNAT), of which three

isoforms have been currently identified. Nicotinic acid phosphoribosyl transferase (NAPT) and nicotinamide phosphoribosyl transferase (NMPT) are key enzymes in the NAD^+ salvage pathway and are responsible for the reutilisation of nicotinic acid and nicotinamide generated by NAD^+ catabolism respectively. Our data shows that QPRT expression is reduced following exposure to UVB in both cell types. This may have a negative effect by limiting NAD^+ anabolism, and enhancing cytotoxicity due to the accumulation of QUIN at pathophysiological concentrations. Increased expression of NAPT and NMPT parallel to a down regulation in QPRT mRNA expression levels suggests that low NAD^+ states such as UVB and/or cytokine mediated inflammation can specifically induce the genes in the NAD^+ salvage pathway when the de novo KP is impaired. This effect is aimed at restoring intracellular NAD^+ levels and maintaining NAD-dependent processes leading to improved cell viability and restoration of normal cellular function.

Several studies have demonstrated that upregulation in the KP and particular the expression of IDO1 may play a critical role in immunomodulation [Munn et al., 1998; Terness et al., 2002]. The immunosuppressive effect of IDO expression on the survival of allo- and xenogeneic skin cells has already been demonstrated [Munn et al., 1998; Terness et al., 2002]. However, the effect of UVB and IFN- γ stimulation on T-cells remains unclear. We hypothesised that activation of the KP following treatment with UVB and IFN- γ might lead to T-cell death due to increased production of cytotoxic metabolites of TRYP e.g. QUIN, 3-HAA etc. Alternatively, TRYP depletion might lead to a reduction in T cell proliferation culminating in apoptotic cell death. Herein, we have shown that IFN- γ, a well-established activator of IDO can reduce membrane integrity of bystander T cells but not fibroblasts and keratinocytes. These findings are in line with a previous study showing that skin cells, but not T cells are resistant to IDO1-induced TRYP depletion [Forouzandeh et al., 2008]. The study showed a significant activation of apoptotic pathways as observed by caspase-3 activation, and increased expression of CHOP, a downstream effector of the general control nonderedpressing-2 (CN2) kinase pathway in T cells, but not in skin cells depletion [Forouzandeh et al., 2008]. However, exposure to UVB significantly reduced the survival rates of all bystander cells, suggesting that UVB may induce cell death via multiple pathways not restricted to KP and GCN2 kinase activation alone.

ROLE OF THE KYNURENINE PATHWAY IN NAD^+ SYNTHESIS IN HUMAN SKIN

In our study, TRYP supplementation induced a dose dependent increase in intracellular NAD^+ levels in fibroblasts and keratinocytes following 24-h incubation, with the most significant increase occurring at a 50 μM concentration. KYN, a metabolite of TRYP reduced NAD^+ levels and cell viability at concentrations when exceeding 0.1 μM in fibroblasts and 10 μM in keratinocytes. As well, NAD^+ levels were not significantly different following administration of varying doses of KYNA in either fibroblasts or keratinocytes. This was expected, as KYNA is not enzymatically catabolised further down the KP. As mentioned earlier, KYNA is an antagonist at glutamate receptors [Perkins and Stone, 1982; Kapoor et al., 1994; Jhamandas et al., 2000] and therefore has protective roles against NMDA receptor-mediated cytotoxicity. Similarly, no change in cell viability was observed in both fibroblasts and keratinocytes following administration of KYNA.

KYN and its downstream metabolite 3-HK can be enzymatically converted to AA and 3-HAA respectively via the catalytic activity of KYNU, which can also potentiate QUIN production [Stone, 2001]. However, AA and 3-HAA do not act in the same fashion as QUIN as

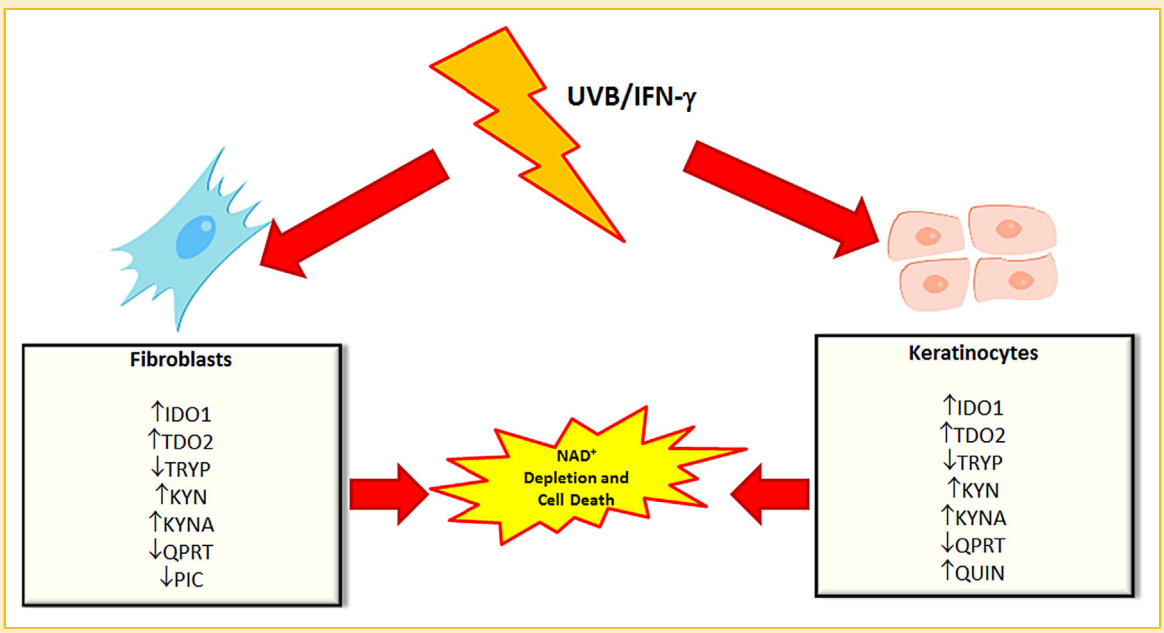

Fig. 11. Summary of the changes in levels of transcripts encoding enzymes in the kynurenine pathway, and the levels of kynurenine pathway intermediates in human skin-derived fibroblasts and keratinocytes following treatment with UVB exposure and/or IFN-γ. Arrows indicate significant up- or down-regulation.

they do not activate NMDA receptors, but rather cause cell damage through free radical formation [Stone et al., 2001]. In our study, NAD^+ depletion occurred in both cell types in response to AA and 3-HAA, while NAD^+ levels and cell viability declined in keratinocytes and fibroblasts in the presence of 3-HK at 1 μM and 10 μM respectively.

NAD^+ levels were increased at different concentrations in fibroblasts (<0.5 μM) and keratinocytes (<10 μM) in response to QUIN treatment. Our results are in agreement with previous studies which show that QUIN is beneficial for NAD^+ synthesis but displays apoptotic behaviour at pathophysiological concentrations [Cammer, 2002; Guillemin et al., 2003]. While PIC is generally considered as a protective metabolite in comparison to QUIN, decreased NAD^+ levels and increased cell death were observed in higher then physiological concentrations (>1 μM) in fibroblasts and >0.5 μM in keratinocytes. Elevated PIC levels have been associated with fatalities in children with cerebral malaria [Medana et al., 2002].

Low NAD^+ in fibroblasts and keratinocytes has been shown to cause an increased susceptibility to UV damage through inhibition of the DNA 'nick' sensor poly(ADP-ribose) (PARP-1) and sirtuins (as NAD^+ is the essential substrate), leading to unrepaired DNA damage and increase in cell death [Beneke et al., 2004]. NAD^+ is also an important substrate for the NAD-dependent sirtuin deacetylase, Sirtuin-1 (SIRT1) [Massudi et al., 2012]. There is now emerging evidence indicating an association between the PARP-1 and SIRT1 pathways, which have been previously independently studied. The decline in NAD^+ and the rise in nicotinamide may downregulate the SIRT1 deacetylase activity [Braidy et al., 2011]. It is likely, PARP-1 mediated NAD^+ depletion, as induced by DNA damage, can modulate SIRT1 protein deacetylation of p53, which plays an invaluable role in DNA repair, via the NAD^+/nicotinamide connection [Kastan et al., 1992; Braidy et al., 2011; Matsumura and Ananthaswamy, 2004]. Hence regulation of intracellular NAD^+ by KP metabolites is increasingly important in skin pathologies and fine control of KP metabolite levels could represent a novel approach to skin cancer prevention and/or therapy where DNA damage and impairments in the repair machinery are prevalent.

CONCLUSION

Our data shows that the KP is fully expressed in human fibroblasts and keratinocytes. Exposure to UVB radiation and/or IFN-γ causes significant changes in the expression pattern of downstream KP metabolites and enzymes (Fig. 11). Exposure to various concentrations of KP metabolites showed marked differences in cell viability and intracellular NAD^+ production, providing support for involvement of the KP in the de novo synthesis of NAD^+ in these skin cells. Future studies of the KP in the skin could incorporate pharmacological interventions to decrease activity of the enzyme KYNU and hence decrease production of toxic downstream metabolites although the impact on the production of the downstream pyridine nucleotide, NAD^+ remains unclear. The feasibility of using downstream KP metabolites to improve NAD^+ levels not only in the skin, but in all KP expressing cells as a therapeutic tool for patients with tumors should be further investigated (Adams et al., 2012). Performing a controlled study in which adult and foetal human keratinocytes and fibroblasts are placed under the same conditions can clarify some of the developmental inconsistencies and provide a basis for future work in this area.

ACKNOWLEDGMENTS

This work has also been supported by the National Health and Medical Research Council, The Curran Foundation (Australia), and by the Rebecca Cooper foundation (Australia). Dr Nady Braidy is the recipient of an Alzheimer's Australia Viertel Foundation Postdoctoral Research Fellowship at the University of New South Wales.

REFERENCES

Adams S, Braidy N, Bessede A, Brew BJ, Grant R, Teo C, Guillemin GJ. 2012. The kynurenine pathway in brain tumor pathogenesis. Cancer Res 72: 5649–5657.

Akazaki S, Imokawa G. 2001. Mechanical methods for evaluating skin surface architecture in relation to wrinkling. J Dermatol Sci 27:5–10.

Asp L, Johansson AS, Mann A, Owe-Larsson B, Urbanska EM, Kocki T, Kegel M, Engberg G, Lundkvist GB, Karlsson H. 2011. Effects of pro-inflammatory cytokines on expression of kynurenine pathway enzymes in human dermal fibroblasts. J Inflamm 8:25.

Ball HJ, Sanchez-Perez A, Weiser S, Austin CJ, Astelbauer F, Miu J, McQuillan JA, Stocker R, Jermiin LS, Hunt NH. 2007. Characterization of an indoleamine 2,3-dioxygenase-like protein found in humans and mice. Gene 396:203–213.

Bauer TM, Jiga LP, Chuang JJ, Randazzo M, Opelz G, Terness P. 2005. Studying the immunosuppressive role of indoleamine 2,3-dioxygenase: Tryptophan metabolites suppress rat allogeneic T-cell responses in vitro and in vivo. Transpl Int 18:95–100.

Bender DA, McCreanor GM. 1982. The preferred route of kynurenine metabolism in the rat. Biochim Biophys Acta. 717:56–60.

Beneke S, Diefenbach J, Burkle A. 2004. Poly(ADP-ribosyl) ation inhibitors: Promising drug candidates for a wide variety of pathophysiologic conditions. Int J Cancer 111:813–818.

Bernofsky C, Swan M. 1973. An improved cycling assay for nicotinamide adenine dinucleotide Anal Biochem 53:452–458.

Boegman RJ, el-Defrawy SR, Jhamandas K, Beninger RJ, Ludwin SK. 1985. Quinolinic acid neurotoxicity in the nucleus basalis antagonized by kynurenic acid. Neurobiol Aging 6:331–336.

Bosco MC, Rapisarda A, Massazza S, Melillo G, Young H, Varesio L, The tryptophan catabolite picolinic acid selectively induces the chemokines macrophage inflammatory protein-1alpha and -1beta in macrophages. J Immunol 1642000; 3283–3291.

Bradford MM. 1976. A rapid and sensitive method for quantitation of microgram quantities of protein utilising the principle of protein-dye binding. Anal Biochem. 53:452–458.

Braidy N, Guillemin GJ, Mansour H, Chan-Ling T, Poljak A, Grant R. 2011. Age related changes in NAD^+ metabolism, oxidative stress and Sirt1 Activity in Wistar Rats. PLOS ONE 6:e19194.

Cammer W. 2002. Apoptosis of oligodendrocytes in secondary cultures from neonatal rat brains. Neurosci Lett 327:123–127.

Chen Y, Guillemin GJ. 2009. Kynurenine pathway metabolites in humans: Disease and healthy States. Int J Tryptophan Res 2:1–19.

Chiarugi A, Meli Moroni EF. 2001. Similarities and differences in the neuronal death processes activated by 3OH-kynurenine and quinolinic acid. J Neurochem 77:1310–1318.

Daubener W, MacKenzie CR. 1999. IFN-gamma activated indoleamine 2,3-dioxygenase activity in human cells is an antiparasitic and an antibacterial effector mechanism. Adv Exp Med Biol 467:517–524.

Fallarino F, Grohmann U, Vacca C, Bianchi R, Orabona C, Spreca A, Fioretti MC, Puccetti P. 2002. T cell apoptosis by tryptophan catabolism. Cell Death Differ 9:1069–1077.

Fernandez PJ, Johnson GS. 1977. Selective toxicity induced by picolinic acid in simian virus 40-transformed cells in tissue culture. Cancer Res 37:4276–4279.

Fujigaki H, Saito K, Fujigaki S, Takemura M, Sudo K, Ishiguro H, Seishima M. 2006. The signal transducer and activator of transcription 1alpha and interferon regulatory factor 1 are not essential for the induction of indoleamine 2,3-dioxygenase by lipopolysaccharide: Involvement of p38 mitogen-activated protein kinase and nuclear factor-kappaB pathways, and synergistic effect of several proinflammatory cytokines. J Biochem 139:655–662.

Forouzandeh F, Jalili RB, Germain M, Duronio V, Ghahary A. 2008. Skin cells, but not T cells, are resistant to indoleamine 2, 3–dioxygenase (IDO) expressed by allogeneic fibroblasts. Wound Repair Regen 16:379–387.

Grant RS, Kapoor V. 1998. Murine glial cells regenerate NAD, after peroxide-induced depletion, using either nicotinic acid, nicotinamide, or quinolinic acid as substrates J Neurochem 70:1759–1763.

Guillemin GJ, Cullen KM, Lim CK, Smythe GA, Garner B, Kapoor V, Takikawa O, Brew BJ. 2007. Characterization of the kynurenine pathway in human neurons. J Neurosci 27:12884–12892.

Guillemin GJ, Kerr SJ, Smythe GA, Smith DG, Kapoor V, Armati PJ, Croitoru J, Brew BJ. 2001. Kynurenine pathway metabolism in human astrocytes: A paradox for neuronal protection. J Neurochem 78:842–853.

Guillemin GJ, Williams KR, Smith DG, Smythe GA, Croitoru-Lamoury J, Brew BJ. 2003. Quinolinic acid in the pathogenesis of Alzheimer's disease. Adv Exp Med Biol 527:167–176.

Guillemin GJ. 2012. Quinolinic acid, the inescapable neurotoxin. FEBS J 279:1356–1365.

Harris CA, Miranda AF, Tanguay JJ, Boegman RJ, Beninger RJ, Jhamandas K. 1998. Modulation of striatal quinolinate neurotoxicity by elevation of endogenous brain kynurenic acid. Br J Pharmacol 124:391–399.

Heyes MP, Brew BJ, Saito K, Quearry BJ, Price RW, Lee K, Bhalla RB, Der M, Markey SP. 1992. Inter-relationships between quinolinic acid, neuroactive kynurenines, neopterin and beta 2-microglobulin in cerebrospinal fluid and serum of HIV-1-infected patients. J Neuroimmunol 40:71–80.

Heyes MP, Ellis RJ, Ryan L, Childers ME, Grant I, Wolfson T, Archibald S, Jernigan TL. 2001. Elevated cerebrospinal fluid quinolinic acid levels are associated with region-specific cerebral volume loss in HIV infection. Brain 124:1033–1042.

Heyes MP, Rubinow D, Lane C, Markey SP. 1989. Cerebrospinal fluid quinolinic acid concentrations are increased in acquired immune deficiency syndrome. Ann Neurol 26:275–277.

Hilmas C, Pereira EF, Alkondon M, Rassoulpour A, Schwarcz R, Albuquerque EX. 2001. The brain metabolite kynurenic acid inhibits alpha7 nicotinic receptor activity and increases non-alpha7 nicotinic receptor expression: Physiopathological implications. J Neurosci 21:7463–7473.

Jacobson EL, Giacomoni PU, Roberts MJ, Wondrak GT, Jacobson MK. 2001. Optimizing the energy status of skin cells during solar radiation. J Photochem Photobiol B 63:141–147.

Jhamandas K, Boegman RJ, Beninger RJ, Bialik M. 1990. Quinolinate-induced cortical cholinergic damage: Modulation by tryptophan metabolites. Brain Res 529:185–191.

Jhamandas KH, Boegman RJ, Beninger RJ, Miranda AF, Lipic KA. 2000. Excitotoxicity of quinolinic acid: Modulation by endogenous antagonists. Neurotox Res 2:139–155.

Kapoor V, Kapoor R, Chalmers J. 1994. Kynurenic acid, an endogenous glutamate antagonist, in SHR and WKY rats: Possible role in central blood pressure regulation. Clin Exp Pharmacol Physiol 21:891–896.

Kastan MB, Zhan Q, el-Deiry WS, Carrier F, Jacks T, Walsh WV, Plunkett BS, Vogelstein B, Fornace AJ, Jr. 1992. A mammalian cell cycle checkpoint pathway utilizing p53 and GADD45 is defective in ataxia-telangiectasia. Cell 71:587–597.

Kerr SJ, Armati PJ, Pemberton LA, Smythe G, Tattam B, Brew BJ. 1997. Kynurenine pathway inhibition reduces neurotoxicity of HIV-1-infected macrophages Neurology 49:1671–1681.

Koh JY, Choi DW. 1987. Quantitative determination of glutamate mediated cortical neuronal injury in cell culture by lactate dehydrogenase efflux assay J Neurosci Methods 20:83–90.

Lee GK, Park HJ, Macleod M, Chandler P, Munn DH, Mellor AL. 2002. Tryptophan deprivation sensitizes activated T cells to apoptosis prior to cell division. Immunology 107:452–460.

Leuthauser SW, Oberley LW, Oberley TD. 1982. Antitumor activity of picolinic acid in CBA/J mice J Natl Cancer Inst 68:123–126.

Li Y, Kilani RT, Rahmani-Neishaboor E, Jalili RB, Ghahary A. 2014. Kynurenine increases matrix metalloproteinase-1 and -3 expression in cultured dermal fibroblasts and improves scarring in vivo. J Invest Dermatol 134:643–650.

Lob S, Konigsrainer A, Zieker D, Brucher BL, Rammensee HG, Opelz G, Terness P. 2009. IDO1 and IDO2 are expressed in human tumors: levo- but not dextro-1-methyl tryptophan inhibits tryptophan catabolism. Cancer Immunol Immunother 58:153–157.

Massudi H, Grant R, Guillemin GJ, Braidy N. 2012. NAD+ metabolism and oxidative stress: The golden nucleotide on a crown of thorns. Redox Rep 17:28–46.

Matsumura Y, Ananthaswamy H. 2004. Toxic effects of ultraviolet radiation on the skin. Toxicol Appl Pharmacol 195:298–308.

Medana IM, Hien TT, Day NP, Phu NH, Mai NT, Chu'ong LV, Chau TT, Taylor A, Salahifar H, Stocker R, Smythe G, Turner GD, Farrar J, White NJ, Hunt NH. 2002. The clinical significance of cerebrospinal fluid levels of kynurenine pathway metabolites and lactate in severe malaria J Biol Chem 269:8128–8133.

Metz R, Duhadaway JB, Kamasani U, Laury-Kleintop L, Muller AJ, Prendergast GC. 2007. Novel tryptophan catabolic enzyme IDO2 is the preferred biochemical target of the antitumor indoleamine 2,3-dioxygenase inhibitory compound D-1-methyl-tryptophan. Cancer Res 67:7082–7087.

Munn DH, Zhou M, Attwood JT, Bondarev I, Conway SJ, Marshall B, Brown C, Mellor AL. 1998. Prevention of allogeneic fetal rejection by tryptophan catabolism. Science 281:1191–1193.

Nahm WK, Philpot BD, Adams MM, Badiavas EV, Zhou LH, Butmarc J, Bear MF, Falanga V. 2004. Significance of N-methyl-D-aspartate (NMDA) receptor-mediated signaling in human keratinocytes. J Cell Physiol 200:309–317.

Noakes R, Mellick N. 2013. Immunohistochemical studies of the Kynurenine Pathway in Morphea. Int J Tryptophan Res 23:97–102.

Okudo S, Nishiyama N, Saito H, Katsuki H. 1998. 3-Hydroxykynurenine, an endogenous oxidative stress generator, causes neuronal cell death with apoptotic features and region selectivity J Neurochem 70:299–307.

Okuno E, Kido R. 1991. Kynureninase and kynurenine 3-hydroxylase in mammalian tissues. Adv Exp Med Biol 294:167–176.

Perkins MN, Stone TW. 1982. An iontophoretic investigation of the actions of convulsant kynurenines and their interaction with the endogenous excitant quinolinic acid. Brain Res 247:184–187.

Sarkhos K, Tredget EE, Li Y, Uludag H, Ghahary A. 2003. Proliferation of peripheral blood mononuclear cells is suppressed by the indoleamine 2, 3-dioxygenase expression of interferon-gamma-treated skin cells in a co-culture system. Wound Repair Regen 11:337–345.

Scott M, Tanguay JJ, Beninger RJ, Jhamandas K, Boegman RJ. 2002. Neurosteroids and glutamate toxicity in fibroblasts expressing human NMDA receptors. Neurotox Res 4:183–190.

Sherin PS, Grilj J, Tsentalovich YP, Vauthey E. 2009. Ultrafast excited-state dynamics of kynurenine, a UV filter of the human eye. J Phys Chem B 113:4953–4962.

GA Smythe, Braga O, Brew BJ, Grant RS, Guillemin GJ, Kerr SJ, Walker DW. 2002. Concurrent quantification of quinolinic, picolinic, and nicotinic acids using electron-capture negative-ion gas chromatography-mass spectrometry Anal Biochem 301:21–26.

Sorensen RB, Kollgaard T, Andersen RS, van den Berg JH, Svane IM, Straten P, Andersen MH. 2011. Spontaneous cytotoxic T-Cell reactivity against indoleamine 2,3-dioxygenase-2. Cancer Res 71:2038–2044.

Spranger S, Spaapen RM, Zha Y, Williams J, Meng Y, Ha TT, Gajewski TF. 2013. Up-regulation of PD-L1, IDO, and T(regs) in the melanoma tumor microenvironment is driven by CD8(+) T cells. Sci Transl Med a116.

Stone TW. 2001. Endogenous neurotoxins from tryptophan. Toxicon 39:61–73.

Stone TW, Darlington G. 2002. Endogenous kynurenines as targets for drug discovery and development. Nat Rev Drug Discov 1:609–620.

Stone TW, Perkins MN. 1981. Quinolinic acid: A potent endogenous excitant at amino acid receptors in CNS. Eur J Pharmacol 72:411–412.

Taniguchi S, Yorifuji T, Hamada T. 1994. Treatment of linear localized scleroderma with the anti-allergic drug, tranilast, Clin. Exp Dermatol 19:391–393.

Terness P, Bauer TM, Rose L, Dufter C, Watzlik A, Simon H, Opelz G. 2002. Inhibition of allogeneic T cell proliferation by indoleamine 2,3-dioxygenase-expressing dendritic cells: mediation of suppression by tryptophan metabolites. J Exp Med 196:447–457.

Thomas SR, Stocker R. 1999. Redox reactions related to indoleamine 2,3-dioxygenase and tryptophan metabolism along the kynurenine pathway. Redox Rep 4:199–220.

Tsentalovich YP, Snytnikova OA, Forbes MD, Chernyak EI, Morozov SV. 2006. Photochemical and thermal reactivity of kynurenine. Exp Eye Res 83:1439–1445.

Tsentalovich YP, Sherin PS, Kopylova LV, Cherepanov IV, Grilj J, Vauthey E. 2011. "Photochemical Properties of UV Filter Molecules of the Human Eye. " Investigative Ophthalmology & Visual Science 52:7687–7696.

Wainwright DA, Balyasnikova IV, Chang AL, Ahmed AU, Moon KS, Auffinger B, Tobias AL, Han Y, Lesniak MS. 2012. IDO expression in brain tumors increases the recruitment of regulatory T cells and negatively impacts survival. Clin Cancer Res.

Yu P, Li Z, Zhang L, Tagle DA, Cai T. 2006. Characterization of kynurenine aminotransferase III, a novel member of a phylogenetically conserved KAT family. Gene 365:111–118.

Yuasa HJ, Takubo M, Takahashi A, Hasegawa T, Noma H, Suzuki T. 2007. Evolution of vertebrate indoleamine 2,3-dioxygenases. J Mol Evol 65:705–714.

Zulian F, Vallongo C, Woo P, Russo R, Ruperto N, Harper J, Espada G, Corona F, Mukamel M, Vesely R, Musiej-Nowakowska E, Chaitow J, Ros J, Apaz MT, Gerloni V, Mazur-Zielinska H, Nielsen S, Ullman S, Horneff G, Wouters C, Martini G, Cimaz R, Laxer R. 2005. Athreya BH; Juvenile Scleroderma Working Group of the Pediatric Rheumatology European Society (PRES) (2005) Localized scleroderma in childhood is not just a skin disease. Arthritis Rheum 52:2873–2881.

SUPPORTING INFORMATION

Additional supporting information may be found in the online version of this article at the publisher's web-site.